Critical Reviews in Biochemistry and Molecular Biology, 27(4,5):403–444 (1992)

Aspects in Structural Studies on Ribosomes

Z. Berkovitch-Yellin

Department of Structural Biology, Weizmann Institute, Rehovot, Israel and
Max-Planck-Research-Unit for Ribosomal Structure D-2000 Hamburg 52

W. S. Bennett

Max-Planck-Research-Unit for Ribosomal Structure, D-2000 Hamburg 52 and
Max-Planck-Institute for Molecular Genetics, Berlin

A. Yonath

Department of Structural Biology, Weizmann Institute, Rehovot, Israel and
Max-Planck-Research-Unit for Ribosomal Structure D-2000 Hamburg 52

Referee: Dr. Wah Chiu, Biochemistry Department, Baylor College of Medicine, Houston, TX

KEY WORDS: ribosomes, crystallography of, image reconstruction of, neutron diffraction of, organo-metallic clusters, undecagold cluster, cryobiocrystallography.

I. INTRODUCTION

The intricate and essential process of the enzymatic translation of the genetic information, encoded in mRNA into proteins, is performed by the universal cellular organelle, the ribosome. Ribosomes from all organisms are assemblies of several strands of RNA and many different proteins. These components are arranged in two subunits of unequal size, which associate upon initiation of protein synthesis. A typical bacterial ribosome contains about one quarter of a million atoms and is of a molecular weight of about 2.3 million Da (1.45 and 0.85 for the large and the small subunits, respectively). About two thirds of the mass of the ribosome is composed of three chains of rRNA, the rest are some 57 different proteins (about 36 in the large and 21 in the small subunit).

Due to the fundamental significance of protein biosynthesis, ribosomes have been the target of a large number of biochemical, biophysical, and genetic studies. These studies have led to an understanding of many functional and evolutionary aspects of protein biosynthesis, provided descriptions of the overall process with varying degree of detail and led to a description of gross structural features, such as spatial *in situ* proximities between several ribosomal components, the secondary structure of ribosomal RNA and approximate localizations of some functional centers (for review see References 1 and 2). At the same time, the many crucial details concerning the accurate molecular mechanism that could not be revealed manifest the acute essentiality of a reliable molecular model of the ribosome.

Single-crystal X-ray and neutron crystallography are currently the only experimental techniques with the potential for yielding reliable molecular models. For macromolecular assemblies of the size of the ribosome, these studies may be supported by three-dimensional image reconstruction from two-dimensional sheets. Though biological macromolecules can dynamically switch among an ensemble of conformational states, the crystallographic analysis usually reveals the structure of only one of the conformations. However, these studies may lead to the definition of a set of conformational states by

1040-9238/92/$.50

comparing independent crystal structures of the same molecule at different environments or in the presence of a variety of ligands.[3] Moreover, a careful investigation of the crystallographic results may lead to the design of additional biochemical experiments that had not been obvious in the absence of this information.

The field of X-ray crystallography has seen major advances in the efficiency of data collection and in the effectiveness of the interpretation of results recently. Nevertheless, for crystallographic studies, the ribosomes are still considered extremely large and complicated. Being ribonucleoprotein complexes that are notoriously flexible, unstable, and routinely prepared as conformationally mixed populations, even their crystallization seemed, until recently, to be a formidable task. On the other hand, natural periodic organization of helices or ordered two-dimensional arrays of ribosomes were observed in eukaryotic cells (e.g., lizard, chicken, amoeba, and human) exposed to stressful conditions, such as suboptimal temperatures, wrong diet, or lack of oxygen. Despite the fact that this organization is induced by internal cellular mechanisms and expressed in only one or two dimensions, some of these ordered forms were suitable for image reconstruction studies at a very low resolution. These studies have yielded some low-resolution albeit useful information about the modes of packing, the interactions between the particles, the outer contour of the ribosomes, and the inner distribution of their components.[4-11]

The observations that ribosomes can be orderly packed and the hypothesis that these ordered forms are the physiological mechanism for temporary storage of ribosomes aimed at preserving their integrity and activity for an expected better future stimulated us to attempt crystallization of ribosomes. We chose to focus our efforts on the crystallization of ribosomes from prokaryotes, as these ribosomes are smaller and have been characterized biochemically in much greater detail than those from eukaryotes. In addition, they can be produced in high purity and large quantities, which is essential for effective crystallographic studies. Moreover, they provide systems for *in vitro* crystallization that is independent of *in vivo* events, environmental influences, and physiological factors that might be difficult or impossible to control and to reproduce.

In this article we describe our advances in both X-ray and neutron crystallography, as well as in image reconstruction of intact, complexed, and modified ribosomal particles. Our efforts to crystallize ribosomes and ribosomal subunits with nonribosomal cofactors and products of protein biosynthesis are an important feature of this work. These efforts are aimed at elucidating the structures of complexes mimicking defined functional states, which may eventually allow the mapping of the different conformations adopted by the ribosome while performing its function. Being of relatively homogenous populations, these complexes should diffract to higher resolution than the crystals of 70S ribosomes as extracted directly from cells in their growth phase with no attempt made to obtain a particular functional state.

II. X-RAY CRYSTALLOGRAPHY

A. The First and Most Crucial Steps: the Preparation of Ribosomes and Their Crystallization

Our initial studies have concentrated on searching for suitable bacterial sources, screening for the right ribosomal particles, and obtaining quality crystals. Extreme care in growing the cells and in the preparation of the ribosomes, coupled with the design of special seeding procedures, led to the growth of several crystal forms, summarized in Table 1. Figure 1 shows some of the different crystal forms that were grown in our laboratories and Table 2 summarizes the crystallographic parameters of those forms that are suitable for crystallographic investigation. As demonstrated, we have been able to grow crystals of naturally occurring and mutated ribosomal particles (complete ribosomes and both subunits) of chemically modified particles by heavy atom clusters and of complexes of ribosomal particles with other components involved in protein biosynthesis: a complex of 70S ribosomes with

TABLE 1
Classification of the Different Crystals of Ribosomal Particles

				Complexes of				
	30S	50S	70S	70S + poly(U)[a]	70S + poly(U) + tRNA[b]	50S + tRNA + nascent chain[c]	mutant (−L11) 50S	mutant (−L11) 70S
E.c.			+					
B.st.	+	+	+			+	+	+
T.t.	+	+	+	+	+			
H.m.	+	+		+		+		

Note: E.c., *Escherichia coli;* B.st, *Bascillus stearothermophilus*; T.t., *Thermus thermophilus*; H.m., *Haloarcula marismortui.*

[a] Complex of 70S ribosomes together with an oligomer of 35 ± 5 uridines serving as mRNA.
[b] Complex of 70S ribosomes together with an average of 1.5 to 1.8 equivalents of $PhetRNA^{Phe}$ and an oligomer of 35 ± 5 uridines, serving as mRNA.
[c] Complex of 50S subunits from *H. marismortui* or *B. stearothermophilus* together with a segment of 18 to 20 mers of poly(Phe) or poly(Lys), respectively, and the corresponding tRNA.

mRNA and about two molecules of charged tRNA and another one of 50S subunits with a nascent polypeptide fragment and a molecule of tRNA.

1. The Correlation between Activity and Crystal Growth

The key for obtaining diffracting crystals from ribosomal particles was the choice of the organism. We obtained our best crystals from particles of halophilic or thermophilic bacteria. Presumably these ribosomes are more stable than those from eubacteria and retain their integrity and activity during the isolation and the crystallization processes. We found a strong correlation between the activity of the ribosomes and the quality of their crystals. We consistently obtain the best crystals from the most active preparations. Furthermore, in all cases, except for occasional mold fragmentation of rRNA, the crystallized material retains its integrity and biological activity for long periods, in contrast to the short lifetime of isolated ribosomes in solution.

Our current preparative techniques and crystallization conditions (Table 3) are sufficiently refined and reproducible that we are able to obtain crystals from virtually all preparations of active particles listed in Table 1. However, some variability in the ribosome preparations evidently still exists, as the exact conditions for the growth of large and well-ordered crystals must still be refined for each ribosomal preparation.[12,13] It is noteworthy that preparations that crystallize well in one form also yield good crystals of other forms. Thus, the basic factors governing the quality of ribosomal crystals seem to be related more to the quality of the preparation of the ribosomal particles than to the choice of the crystallizing agent.

In contrast to the marked tendency of the large ribosomal subunits to crystallize (Tables 2 and 3), significant difficulties have been encountered in crystallization of small subunits. These difficulties probably originate from the relative instability of these particles, compared with 50S subunits from the same organism. Supporting evidence has been obtained in our laboratories by exposing 70S ribosomes from *E. coli* to proteolytic enzymes from *Aspergillus oryzae*. Large differences in the resistance of the two subunits were observed; the 50S subunits remained intact, while the 30S subunits were completely digested.[14] Therefore, although we obtained crys-

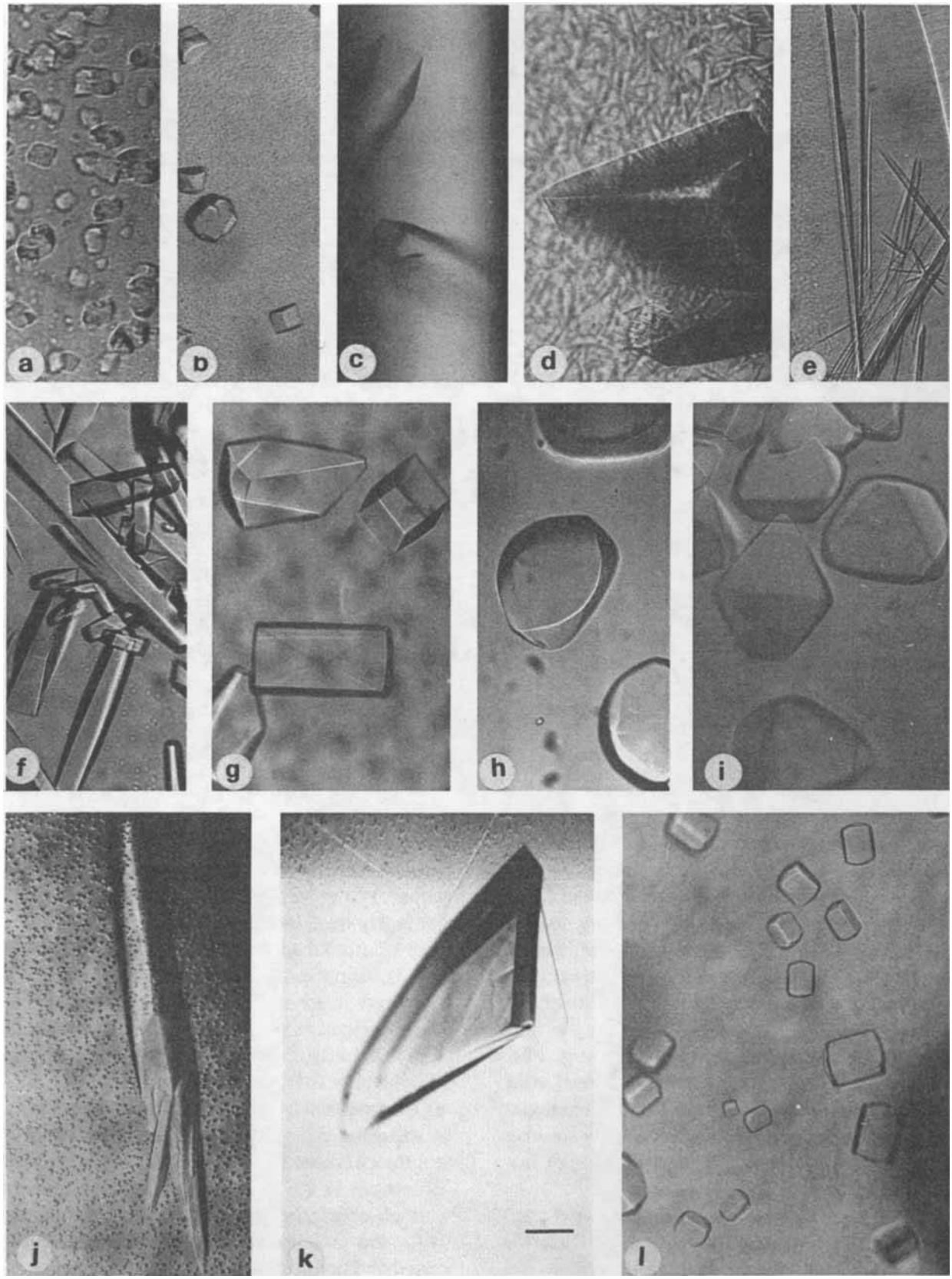

FIGURE 1. Typical crystals of several crystal forms of ribosomal particles (names and growth conditions are as in Table 3 or in the numbered references). Top panel: *B. stearothermophilus*, (a) B30S; (b) B50S (c) B50S(I); (d) B50S(II); (e) B70S; middle panel: *T. thermophilus*, (f) T30S; (g) T50S; (h) T70S(I); (i) T70S(I) complexed with mRNA (35 mers polyuridine) and two (phe)tRNA^{phe}; bottom panel: *H. marismortui*, (j) H30S; (k) H50S(I); (l) H50S(II).

TABLE 2
Characterized Three-Dimensional Crystals of Ribosomal Particles

Source	Grown from	Cell dimensions (Å)	Resolution (Å)
70S T.t	MPD[a]	524 × 524 × 306; $P4_12_12$	App. 20
70S T.t + m-RNA, and t-RNA[b]	MPD	524 × 524 × 306; $P4_12_12$	App. 15
30S T.t.	MPD	407 × 407 × 170; $P42_12$	7.3
50S H.m.	PEG[a]	210 × 300 × 581; $C222_1$	3.0
50S T.t.	AS[a]	495 × 495 × 196; $P4_12_12$	8.7
50S B.st.[c]	A[a]	360 × 680 × 920; $P2_12_12$	App. 18
50 B.st.[c,d]	PEG	308 × 562 × 395; 114°; C2	App. 11

Note: B.st, *Bascillus stearothermophilus*; T.t., *Thermus thermophilus*; H.m., *Haloarcula marismortui.*

[a] MPD, PEG, A, As, crystals were grown by vapor diffusion in hanging drops from solutions containing methyl-pentane-diol (MPD), polyethyleneglycol (PEG), ammonium sulfate (AS), or low-molecular-weight alcohols (A).

[b] A complex including 70S ribosomes, 1.5 to 2 equivalents of $PhetRNA^{Phe}$, and an oligomer of 35 ± 5 uridines serving as mRNA.

[c] Same form and parameters for crystals of large ribosomal subunits of a mutant (missing protein BL11) of the same source and for modified particles with an undecagold-cluster.

[d] Same form and parameters for crystals of a complex of 50S subunits, one tRNA molecule and a segment (18 to 20 mers) of a nascent polypeptide chain.

tals of 30S subunits from three bacteria (Tables 1 and 3), so far the only crystals usable for crystallographic studies are of 30S ribosomal subunits from a highly thermophilic bacteria, *Thermus thermophilus*,[15-17] which is also the source for similar crystals grown in other laboratories.[18,19]

2. Systematics in Crystal Growth

The growth of diffracting crystals was a result of a careful and systematic exploration of the factors influencing crystallization, coupled with the introduction of an innovative experimental procedure for fine control of the volume of the crystallization medium.[20] The crystals of the 50S subunits from *Bacillus stearothermophilus* were the subject of the most thorough analysis of the parameters that control the growth of ribosomal crystals. Three different crystallization devices allowing vapor diffusion were assembled: hanging drops on glass surfaces placed on petri dishes, liquid columns in X-ray capillaries placed in long glass cylinders, and multiple depression plates.[20] In this analysis all the crystallizing droplets contained only the ribosomal subunits and a buffer for controlling the pH. These were equilibrized with low-molecular-weight organic solvents, which were chosen as crystallization agents due to their contribution to the recovery of partially damaged ribosomes.[21]

Among the variables that have been screened were the crystallization agent, pH, chemical nature of the buffer, content of the reservoir, concentration of the ribosomal particles, and the nature of the organic solvents. Both volatile (those whose vapor pressure is higher than that of water) and less volatile compounds (of vapor pressure equal or lower than that of water) were used. In principle, volatile organic solvents should lead to an increase of the volume of the droplets, whereas the opposite effect is expected with less

TABLE 3
Conditions for Crystallization of Ribosomal Particles

Source	Buffers	Final Concentrations of crystallizing agents	Comments and Ref.
E. coli			
70S	H-I; bpH = 7.8	12% MPD	29
B. Stearothermophilus			
B30S	TM, bpH = 6.8	0.5 *M* KCl; 0.18 *M* NH_4Cl; 0.03 *M* $MgCl_2$; 0.002 *M* OG; 0.002 HT 2.5% PEG (20 K)	13
B50S (I)	H-I; bpH = 8.8	12% methanol; 12% ethylene glycol	35–38 (Grown in X-ray capillaries at 4°C with no seeding)
B50S (II) B50S (TST) B50S (GC)	TM, bpH = 6.6	0.8 *M* KCl; 0.05 *M* NH_4Cl; 0.03 *M* $MgCl_2$; 2.5% PEG (6 K)	32, 40
B70S	H-I; bpH = 5.9	0.98 *M* KCl; 0.5 *M* As; 0.01 $MgCl_2$; 0.002 OG; 2.5% PEG (10 K)	13, 28
H. marismortui			
H30S	Hm; bpH = 5.6	2 *M* KCl; 0.5 *M* NH_4Cl; 0.1 *M* $MgCl_2$, 0.005 *M* $CdCl_2$ or $CoCl_2$; 7% PEG (6 to 8 K)	13
H50S (I), H50S (I) with nascent polypeptide	Hm bpH = 5.6	1.6 to 1.8 *M* KCl; 0.5 *M* NH_4Cl; 0.05 *M* $MgCl_2$, 7% PEG (6 to 8 K)	44, 49
H50S (I,Cd)	Hm, bpH = 5.6	1.6 to 1.8 *M* KCl; 0.5 *M* NH_4Cl; 0.05 *M* $MgCl_2$; 0.001 *M* $CdCl_2$; 7% PEG (6 to 8 K)	50
H50S (II)	Hm; bpH = 5.6	1.4 *M* KCl; 0.5 *M* NH_4Cl; 0.05 *M* $MgCl_2$; 7% PEG (6 K) 0.001 *M* OG	Grown in "sitting drops" dialyzed against the reservoir 50
T. thermophilus			
T30S T30S (GC)	$H_{10}M_{10}N_{60}$	12 to 18%; 0.01 *M* spermidine	16, 33
T50S	$H_{10}M_{10}N_{60}$ bpH = 5.6	1.6 *M* As; 0.1% PEG (6 K)	46
T70S (I) and its complexes with: (a) 35 mers poly(u) (b) 35 mers poly(u) and 2 phetRNA^{Phe}	$H_{10}M_{30}N_{60}$	11 to 13% MPD	28, 45
T70S (II)	$H_{10}M_{30}N_{60}$	3% PEG (6 K) 0.001 *M* $CdCl_2$	

TABLE 3 (continued)
Conditions for Crystallization of Ribosomal Particles

Note: (1) For obtaining good crystals, the ribosomal particles must be active in biosynthesis. Usually, better crystals were obtained after a short activation of the material (5 to 10′ at 40 to 60°C). (2) In all cases best crystals are obtained from solutions containing 4 to 15 mg/ml (80 to 300 A_{260}/ml) ribosomal particles. (3) The crystallization conditions were chosen to be as similar as possible to the natural environment. (4) In all cases large crystals were obtained by vapor diffusion. The method of the "hanging drop" in Linbro dishes with drops of 5 to 7 μl and a reservoir of 1 ml was usually used. Exceptions: B50S (I) from which the best crystals were obtained in X-ray capillaries (drop = 25 μl; reservoir = 10 ml) and H50S (II), which grew in sitting drops dialyzed against the reservoir. (5) In all cases spermine or spermidine can be added to the crystalline mixture. In no case was there any improvement or change in the quality of the crystals caused by the presence of these polyamines. (6) When organic materials are used as crystallization agents, no crystals grew when there was an expansion of the volume of the drop. To avoid this, 0.8 to 1.0 *M* NaCl was added to the reservoir (Yonath et al., 1982a). (7) Unless otherwise mentioned, the crystals grew at 19°C. (8) Unless otherwise mentioned, large crystals grew only by individual seeding. (9) So far, for all cases, the lower the Mg^{2+} concentration the thicker the crystals.

Abbreviations: H-I: 10 m*M* hepes, 60 m*M* NH_4Cl, 10 m*M* $MgCl_2$, 6 m*M* mercaptoethanol, pH = 7.5; TM: 20 m*M* tris, 10 m*M* $MgCl_2$, 8 m*M* mercaptoethanol, pH = 8.0; Hm: 1.2 *M* CKl, 0.5 *M* NH_4Cl, 0.05 *M* $MgCl_2$, 0.002 *M* tris HCl, pH = 8.0; $H_{10}M_{10}N_{60}$: 10 m*M* hepes; 10 m*M* $MgCl_2$; 60 m*M* NH_4Cl; pH = 7.8; $H_{10}M_{30}N_{60}$: 10 m*M* hepes; 30 m*M* $MgCl_2$; 60 m*M* NH_4Cl; pH = 7.8; bpH is the pH buffer: 0.02 to 0.1 *M* of the following list added to the solution of the ribosomal particles in their storage buffer:

Acetate (pH = 4 to 6)	MES (pH = 6 to 7.2)
Hepes (pH = 7.2 to 8.5)	glycine (pH = 8.5 to 10)

MPD: 2-methyl-2,4-pentanediol; OG: octyl-β-D-glycoside; HT: heptantriol; PEG: polyethyleneglycol; AS: ammonium sulfate; GC: undecagold cluster; TST: a mutant of *B. stearothermophilus*, missing protein L11.

volatile solvents. Unexpectedly, for all organic solvents we observed an unusual expansion of the volumes of crystallization droplets.[20] We assumed that this may result from specific interactions between the ribosomal particles and the organic solvents. Evidence has been obtained that ribosomes are highly hydrated and that the hydration shell is made up of two components, one of which is bound tighter than the other.[116] The organic solvent may replace some of the bound water by specific binding to the ribosomal particles. The growth of crystals from water-insoluble organic solvents supports this view, since most of the crystals were found on the surface of the drop where the ribosomal subunits could interact directly with the vaporized solvent.

The very first indications for crystallization were obtained when less volatile solvents (such as 2-methyl-2,4-pentane diol (MPD), ter-butanol, or toluene) were used.[22] These caused a somewhat limited expansion of the volume of the crystallization droplet when compared with that produced by the volatile solvents. Therefore, we associated the appearance of crystals with mild or no expansion of the droplet, and searched for conditions that would reduce the amount of expansion, or, preferably, decrease the volume of the droplet. An experimental procedure for a fine control of the volume of the droplet was thus developed, aimed at reaching the right conditions for crystallization in the early stages of the experiment before the ribosomal subunits become

inactive and lose their ability to crystallize. The procedure is based on addition of an inert inorganic salt to the reservoir. Employing this procedure, contraction of 6 to 10% of the volume of the droplet was achieved within the first few days, and thereafter the volume remained almost constant for weeks.

The failure to crystallize could not be simply attributed to dilution of the 50S subunits caused by the expansion of the droplet, since we have shown that crystallization occurred over a wide range (1 to 25 mg/ml) of initial concentrations of the subunits.[20] Therefore, we connected the ability to crystallize with the particular distribution of the subunits within the droplet during the critical initial period of the crystallization experiment (see Section II.A.3 and Reference 23). Thus, an early addition of salts to the reservoir could facilitate crystal growth, whereas late addition has no positive influence on crystallization.

In later experiments, the quality and size of the crystals were improved significantly by the development of a device in which crystallization takes place in X-ray capillaries (Figure 2). The special geometry of this crystallization device was designed to facilitate the production of fewer and larger crystals. Since X-ray capillaries are very thin and sealed at the bottom and since they are placed so that their open ends are far from the reservoir, this device provides a series of physical bottlenecks for a free movement of vapor, thus retarding the equilibration of the crystallization column with the reservoir. Of particular importance are the relatively large volume of the crystallization chamber, the long distance between the crystallization media and the reservoir, the small air-exposed surface area of the crystallization droplets and the dynamics of the diffusion of the crystallization agent through the long and narrow crystallizing column. As crystallization occurred even when non-water-miscible volatile materials were used, we assumed that the nucleation of crystals starts on the interface between the droplet and the air. Furthermore, we have found evidence for a reciprocal correlation between the size of the air-exposed surface area of the crystallizing drop and the number and the size of grown crystals. Indeed, decreasing the size of the surface area available for nucleation resulted in the production of fewer but larger crystals.

The growth of large crystals in the capillaries can also be linked to the kinetics of diffusion of the organic solvent within the long and narrow droplet. The same typical pattern of crystal growth was observed in almost every capillary, regardless of the type and the source of the ribosomal particles and of the crystallizing agent. The typical average size of the crystals was found to be correlated with the location along the crystallizing column (Figure 2, middle). In general, we first observed a large number of rather small crystals near the top end of the column near the interface with the air. A smaller number of very large crystals (with length up to 2 mm) were grown in the middle of the column. The bottom end was usually full of fragments of crystals that sank because they were too heavy to be held to the wall of the capillary by surface tension.

3. The Nucleation of Crystals of Ribosomal Particles

The process of crystal growth is initiated by nucleation. Although many biological macromolecules and assemblies have been crystallized, little is known about the mechanism of nucleation. Approximate theoretical models[24,25] have been developed for explaining the nucleation of crystals of small molecules, but only a few of them apply to biological macromolecules. Most of the data currently available concerning nucleation of crystals of biological systems are based on rather indirect evidence, such as use of scattering techniques for monitoring the size of readily formed aggregates.[26]

The crystals of ribosomal particles provide an excellent system for direct investigation of nucleation because the individual particles are large enough to be seen by electron microscopy. We took advantage of the tendency for crystallization of 50S subunits from *B. stearothermophilus* to follow the initial steps in the formation of crystals.[23] For these experiments the crystallization process was interrupted before the growth of mature crystals, and the crystallization medium was either spread on electron microscopy

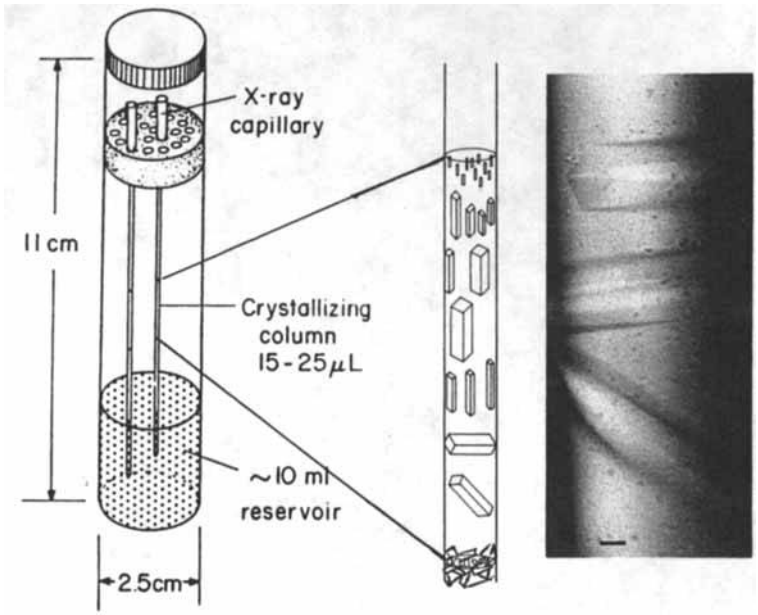

FIGURE 2. Left: the crystallization device that was used for growing crystals by vapor diffusion in X-ray capillaries.[12,20] Middle: a graphical representation of a typical distribution within the crystallization column. Right: three crystals grown at the lower part of the X-ray capillary. (Bar = 0.1 mm.)

grids and stained negatively or cross-linked with glutaraldehyde, embedded in epon, sectioned, positively stained, and examined by electron microscopy. It was observed that the process of crystal growth starts within a rather short time (6 to 72 h) by nonspecific aggregation (Figure 3). We believe that this immediate nonspecific aggregation, induced by the crystallization agents, inhibits the natural tendency of ribosomal particles to disintegrate in solution. It is likely that nucleation of ordered crystals starts within the amorphous aggregates, as almost no single particles could be detected on micrographs, regardless of glutaraldehyde fixation. In later stages and under favorable conditions, these aggregates undergo rearrangements toward the formation of three-dimensional crystals. Thus, we believe that the nucleation of crystals of ribosomal particles is not a result of collision between single particles in the solution, but occurs within the preformed amorphous aggregates. This hypothesis accords well with our observation that the dynamic processes that take place in the initial stages of crystallization have a significant influence on the mere appearance of crystals. We have observed that during this period even a slight expansion of the volume of the crystallization drop may prohibit the production of crystals.[20]

The surface of the ribosome is a composite of a variety of potential interaction sites, some of which are suitable to form interparticle contacts that may lead to the production of various periodic structures, whereas the others are capable of forming contacts of relatively weak binding energies. Indeed, a few of the nucleation centers have the same morphology as that of the three-dimensional mature crystals, whereas others form star-shaped crystallites or helical arrangements (Figure 3). The nucleation centers of both the proper and the non-proper crystals appear to be reasonably well formed, but exhibit different patterns and repeating distances. The formation of star-like nuclei that may originate from a multidirectional growth may point at an inherent characteristic of ribosomes. This may also be the cause for the extreme sensitivity of the crystallization process to small changes in external conditions, for the high mosaicity of the three-dimensional crystals, and for the difficulties encountered in obtaining larger crystals. The

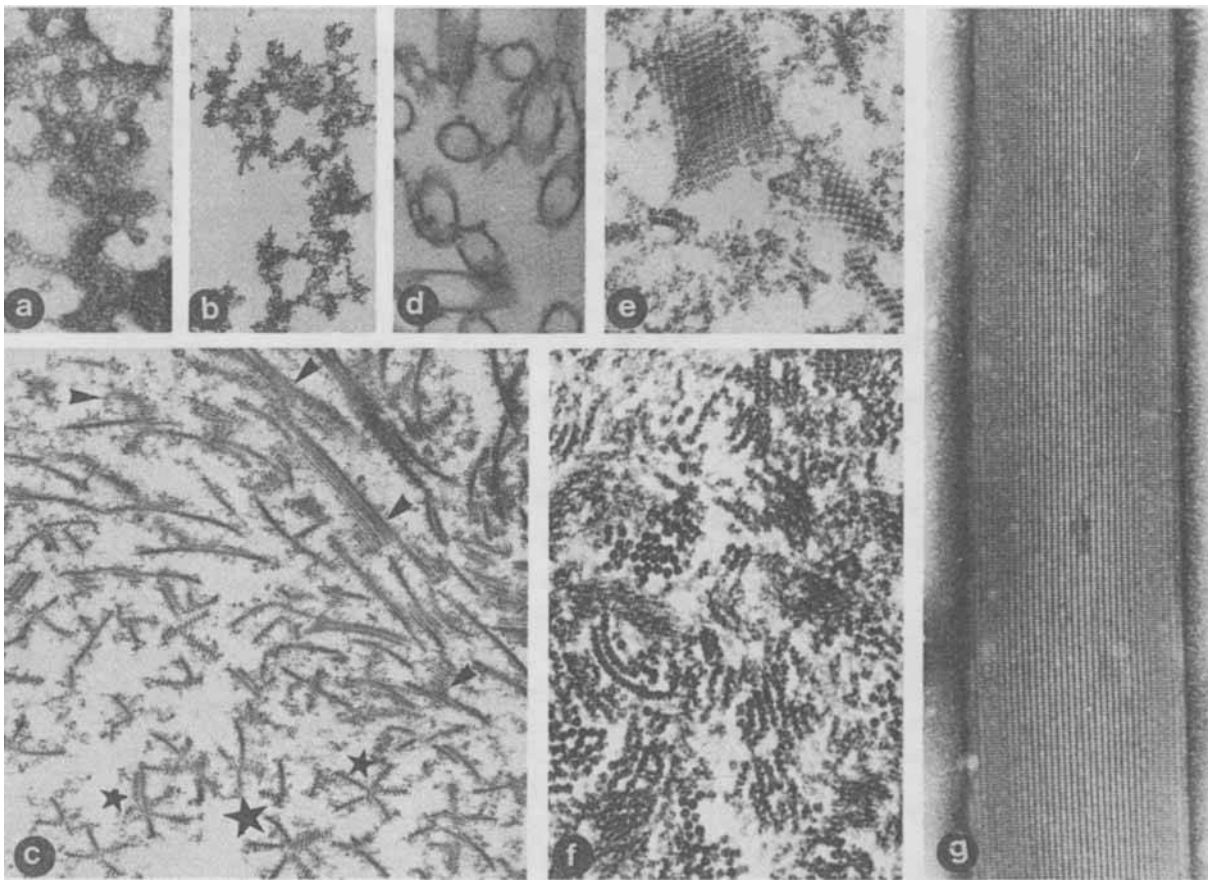

FIGURE 3. The nucleation of crystals of (a to e) 50S ribosomal subunits from *B. stearothermophilus*, and of 70S ribosomes from *E. coli* (f), and from *T. thermophilus* (g), as detected by electron microscopy. (a) The content of the crystallization droplet containing 50S subunits at pH = 6.6, equilibrated with its reservoir of 10% ethyleneglycol for 5 d, applied to a grid and negatively stained with 1% uranyl acetate; (b to g) thin sections through cross-linked and embedded droplets. The growth conditions of (b, c) are as for (a), the arrows point at potential proper crystals, the stars mark a star-like growth. The growth conditions of (d) are 10% ethanediol and 5% hexanediol, pH = 7.2; (e, f) were grown in X-ray capillaries, equilibrized with 30% methanol at pH = 6.3, and 12% MPD, pH = 7.8, respectively; (g) shows a section through a mature, large crystal, obtained after 20 d. All experiments except for g were performed at 4 to 9°C. The exact experimental details for a to d are given in Reference 23, for e in Reference 34 (form 3), for (f) in Reference 29, and for g in Reference 95, but without KCl.

high degree of polymorphism may also be correlated to the large conformational hetrogenicity of the ribosomal particles. Thus, it is not surprising that several different crystal forms were developed under similar crystallization conditions, and that small variations in the crystallization medium may introduce large differences in the crystallographic constants. Appropriate examples are the six crystal forms of 50S subunits from *B. stearothermophilus*;[13,17] the five forms of 50S subunits from *Haloarcula marismortui* (see below, Section II.B.3); and the difference of about 65 Å in one cell axis of the MPD-grown crystals of 70S ribosomes from *T. thermophilous*, which resulted from the presence of 0.2 *M* KCl in the crystallization buffer.[15,18,27,28]

B. Bacterial Ribosomes As Seen by the Crystallographer

1. E. coli

By far, the best biochemically characterized bacterial ribosomes are those of *E. coli*. For this reason, we as well as others have invested con-

siderable effort in attempts to crystallize these ribosomes. Unfortunately, ribosomes from this source are rather unstable and could not be maintained intact for the periods needed for the production of large crystals. Therefore, only microcrystals could be grown.[29] These were suitable for electron-microscopical diffraction studies of positively stained thin sections of epon-embedded crystals (see below, Section IV.A.1 and in Reference 30).

2. Thermophilic Bacteria

In contrast to the poor results in the crystallization of ribosomal particles from *E. coli*, we obtained crystals of all three naturally occurring ribosomal particles (30S, 50S, and 70S) from two thermophilic bacteria, *B. stearothermophilus* and *T. thermophilus* (Tables 1 to 3).

a. Bacillus stearothermophilus

The ribosomes of the moderate thermophile, *B. stearothermophilus*, are rather well characterized by chemical, physical, and immunological methods (for review see References 1 and 2) and thus are rather attractive for structural studies. Of particular interest is the possibility of obtaining, by thiostrepton mutagenesis, ribosomes missing protein BL11.[31] These mutated ribosomes are suitable for the production of specific heavy-atom derivatives, which may be useful for phasing of X-ray diffraction data (see below, Section III.A and in References 32 and 33).

As mentioned above, the 50S subunits from this bacterium were the first ribosomal particles of be crystallized.[22] The initially grown microcrystals that were not suitable for single-crystal crystallographic studies played a crucial role in the progress of our work, since their diffraction patterns contained features, such as arcs and rings, with spacings up to 3.5 Å resolution.[22] Encouraged by the appearance of these microcrystals and by their potential internal order, we pursued further intensive crystallization experiments, which within a few years yielded crystals suitable for crystallographic studies.

Using this bacterium, we succeeded in growing seven crystal forms of the 50S subunits,[13,17,34–43] one of the 30S subunits[13] and one of whole 70S ribosomes,[13,28] under a variety of conditions (Table 3). Except for two forms (designated as B50S(I) and (II) in Table 3), of which the latter can be studied at medium resolution (Table 2 and in References 35 to 43), these crystal forms are not suitable for crystallographic analysis. It is of interest that the same crystallization conditions that yielded the two forms suitable for crystallographic analysis also produced crystals of mutated, reconstituted and derivatized subunits.[32,38,40,41] Furthermore, the same crystallization conditions were found suitable for obtaining crystals from complexes of these subunits with tRNA and short nascent polypeptide chains[44] and all crystals grown under the same crystallization conditions appeared to be isomorphous with the native ones.[13]

Because ribosomes from eubacteria tend to disintegrate at high salt concentrations and to precipitate at low polyethyleneglycol (PEG) concentrations, we first used low-molecular-weight organic materials as crystallization agents. As mentioned above, these are also attractive due to their positive effect in reactivation of slightly damaged ribosomes.[21] Reasonably good crystals were obtained when low-molecular-weight alcohols, methanol, and ethyleneglycol were used (form B50S(I) in Table 3 and in References 13 and 35 to 38). Mg^{2+} was found to play a major role in the crystallization of ribosomal particles, and we have investigated the formation of three-dimensional crystals as a function of its concentration in the crystallizing drop. Preparations, which at relatively low (5 to 25 m*M*) Mg^{2+} concentrations produced normal three-dimensional crystals, were tested for crystal growth over a wider range of Mg^{2+} concentrations. It was found that when the concentration of Mg^{2+} exceeds a critical value (about 100 m*M* for B50S(I)), in most cases no three-dimensional crystals could be detected by light microscopy. In only a few experiments were small three-dimensional crystals produced, but these dissolved within 1 to 2 d. Further, it was found that the upper critical value of Mg^{2+}, which is permitted for the production of three-dimensional crystals, is the lowest needed for the growth of two-dimensional sheets. It appears that Mg^{2+} has the potential to

inhibit the growth along the direction perpendicular to the main plan of the sheets, but does not effect or even enhance the intraplaner growth.

Unfortunately, even the large crystals (up to 1.2 mm in length) obtained from alcohols were only marginally suitable for crystallographic studies, since any handling of the crystals or replacing the growth medium with a different solution were virtually impossible. To overcome these severe shortcomings we grew the crystals directly in X-ray capillaries (see above, Section II.A.2 and below, Section II.C.2) and, in parallel, initiated an intensive search for alternative crystallization agents. The latter led to the growth of well-formed crystals from solutions containing low concentrations of salts, closely resembling the natural environment of the ribosomes within the living cells, with the addition of minute amounts of PEG (form B50S(II) in Table 3).

Although subsequently we were able to grow crystals of 50S ribosomal subunits from other bacteria (*H. marismortui* and *T. thermophilus*) that diffract to higher resolution, the crystals of the 50S subunits from *B. stearothermophilus* may still play a unique role in the crystallographic structure determination. As described below (Section III.A) and seen in Tables 1 and 2, we were able to obtain from this source a single-site derivative, which should be suitable for phasing, as well as by the unambiguous location of its binding site.

b. Thermus thermophilus

The ribosomes of the extreme thermophile *T. thermophilus* are rather poorly characterized biochemically, but because of the growing general interest in thermal stability of biological macromolecules intensive biochemical studies of ribosomes from this species have been initiated in several leading laboratories.

All naturally occurring ribosomal particles from this bacterium yielded crystals suitable for crystallographic analysis at medium or low resolution (Tables 1 to 3 and in References 16 to 19, 27, 28, 45, and 46). Thus, crystals of ribosomal particles from this bacterium provide a set that may be suitable for detecting gross conformational changes correlated with subunit association, as well as large conformational changes expected to accompany translocation and other steps in the process of protein biosynthesis (see below, Section V).

So far, all crystals of the entire 70S ribosome (from *E. coli, B. stearothermophilus*, and *T. thermophilus*) consistently diffract to low resolution. Given the correlation that we have observed between the activities of samples of 30S or 50S subunits and the quality of the crystals obtained from them, we believe that the poor internal order of the crystals of 70S particles is due to inherent conformational and/or functional heterogeneity of the 70S tight couples used for crystallization.

We reasoned that 70S ribosomes, reassembled from purified 50S and 30S subunits, might provide a rather homogeneous population of ribosomes that should, in turn, form more ordered crystals. A highly active hybrid of 50S subunits from *B. stearothermophilus* and 30S subunits from *E. coli* was prepared and its crystallization was attempted in media similar to that used for *in vitro* poly(U)-programmed polyphenylalanine synthesis. Large and well-ordered crystals were obtained. However, sucrose gradients of dissolved crystalline material showed that these crystals contained only 50S subunits.[13,28] This result is consistent with our previous observations that the 50S ribosomal subunits crystallize readily under a variety of conditions (Table 1; References 17, 22, 30, 34 to 44, and 46 to 50) and indicates that the interparticle interactions in the crystals of the large subunits are stronger than the affinity between the large and small subunits in hybrid 70S particles left for relatively long periods without being activated in protein biosynthesis. It is noteworthy that similar observations have been made for packed two-dimensional sheets of two types of eukaryotic 80S ribosomes, of oocytes,[10] and in brains of senile people.[8] Such sheets could artificially (first example) or naturally (the second example) be depleted of the small subunits and still maintain their packing integrity in a lattice composed of only large subunits.

Of particular interest are the crystals of complexes of 70S ribosomes with two other components that participate in protein biosynthesis, mRNA, and tRNA (Tables 1 and 2). Crystals containing an oligomer of about 35 uridines and

approximately two tRNA charged molecules diffract better than any other crystals of 70S particles that we or others have obtained so far.[13,18,27,28,45] A further improvement of the resolution is expected from crystals of 70S ribosomes programmed with mRNA of selected sequences.

3. Haloarcula marismortui

The Dead Sea, which has the highest salt concentration of any natural body of water in the world, unexpectedly supports the growth of several species of microorganisms, all of which exhibit the unusual property of withstanding high salt concentrations. One of these is the archaebacterium *H. marismortui*. Experience showed that nonribosomal proteins purified from these bacteria could be crystallized.[51,52] We have isolated the halobacterial ribosomes and their subunits and found that although at least 2.5 *M* KCl and 0.5 *M* of ammonium sulfate are required for their activity in protein biosynthesis they maintain their integrity over a wide range of salt concentrations.[47] Consequently, we have developed a procedure that allows the crystallization of halophilic ribosomal particles in solutions with the lowest concentrations of salts essential to avoid dissociation.[47] However, the crystallographic studies were performed on crystals soaked in solutions of composition similar to the physiological environment within the cell of this bacterium in which the full biological activity of these ribosomes is retained (Figure 4).

Five crystal forms of 50S subunits and one of the 30S subunits from *H. marismortui* were obtained by us (Tables 1 to 3 and in References 13, 17, and 47 to 50). Of particular interest are those named H50S(I) and its improved version, H50S(I,Cd) in Table 3 and in References 49 and 50, which are most valuable, as they diffract to the highest resolution obtained by us so far, 3 Å (Figure 4 and Table 2). This rather impressive resolution limit was reached recently, after extensive refinements of conditions, the introduction of sophisticated seeding procedures,[12,42,43,49] and a systematic search for an appropriate additive, which was found to be Cd^{2+} to the crystallization mixtures.[50]

In searching for optimal conditions for crystal growth, we were guided by the complementary effects of the concentrations of monovalent and divalent ions on the growth of halobacteria, as well as by the role played by the Mg^{2+} concentration in crystallization of all ribosomal particles. We have found that for spontaneous growth of crystals of ribosomal particles, lower Mg^{2+} concentrations tended to yield thicker crystals. An extreme example of this effect is provided by 50S subunits from *B. stearothermophilus*, which crystallize in three dimensions at a relatively low Mg^{2+} concentration, whereas at a higher Mg^{2+} concentrations two-dimensional sheets are formed (Reference 53, see also above, Section II.B.2.a and below, Section IV.A.2). Similarly, we found that for the 50S subunits of *H. marismortui*, the spontaneously grown crystals at the lowest possible Mg^{2+} concentration, are quite thin, but can be used to seed solutions of 50S subunits with slightly lower concentrations of Mg^{2+}. The seed crystals appear initially to dissolve, but after about 2 weeks thicker, well-ordered crystals are formed.[12,49]

The influence of Mg^{2+} on the quality of the crystals may be partially attributed to its contribution to the integrity of the ribosomal particles. However, even optimal Mg^{2+} concentrations could not lead to the effect obtained by the addition of 1 m*M* Cd^{2+}, namely, the reproducible growth of crystals diffracting to 3 Å resolution with a reasonable mosaicity and superb mechanical stability.[50]

The interest in the third crystal form, named H50S(II) in Table 3, is due to the correlation between its morphology (Figure 1) and the additive. As seen in Table 3, the composition of the crystallization media of this form is essentially identical to that of H50S(I), except for the addition of a tiny amount of β-octyl-glucoside, which caused significant morphological changes in a yet not understandable fashion but similar to observation made in crystallization of isolated proteins[54] as well as of small organic molecules.[55] It is noteworthy that the addition of tiny amounts of this compound alone or together with Cd^{2+}

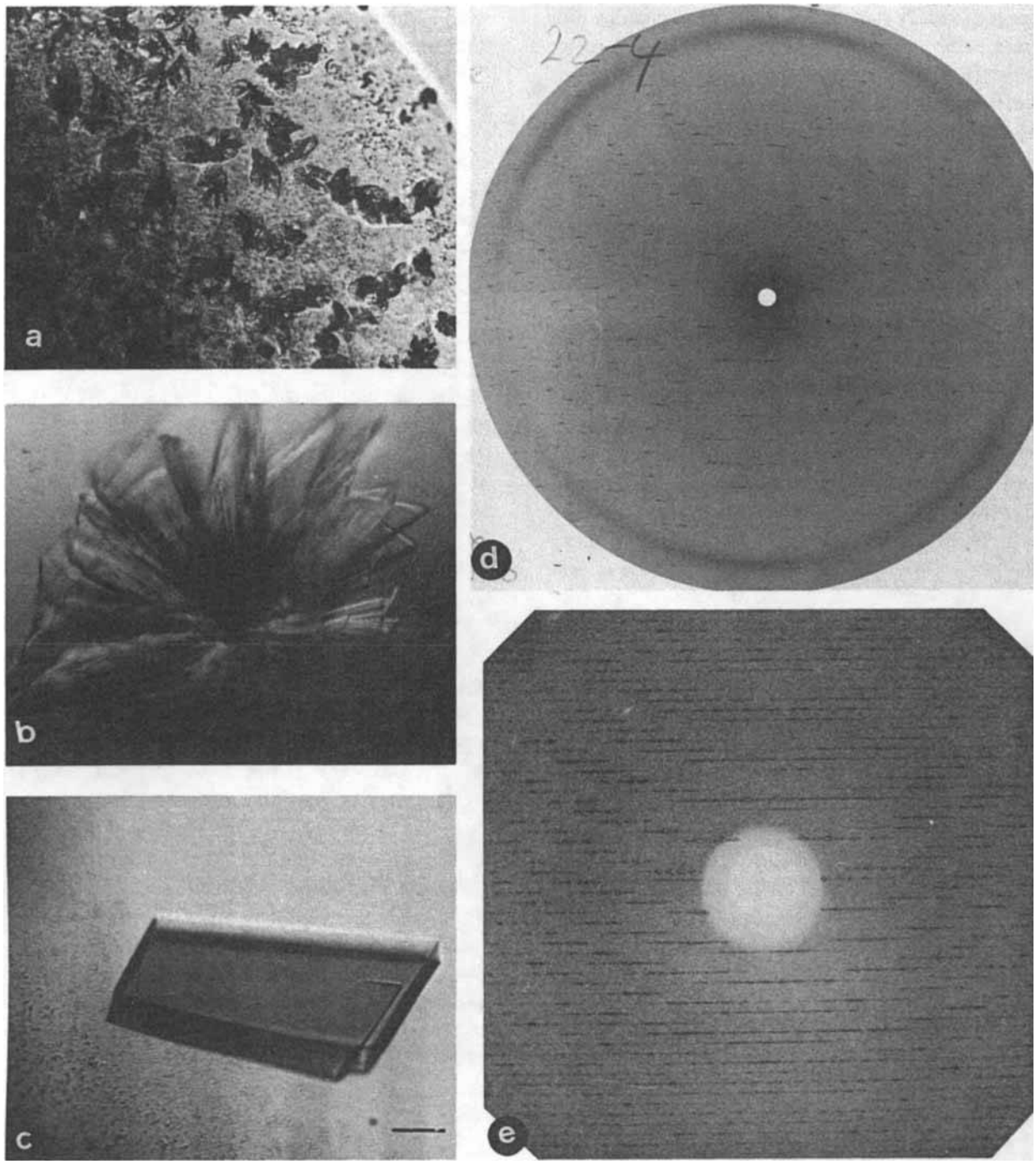

FIGURE 4. Crystals of 50S subunits of *Halobacterium marismortui*: from the initial (a) to (c) H505(1) Growth conditions: (a) as in Reference 47, (b) as in Reference 48, (c) is H50S(I) in Table 3, grown from a solution containing the minimum amount of salts needed for maintaining the integrity of the halophilic ribosomes[47,49] by individual seeding.[12,43] (d, e) X-ray diffraction patterns (1° rotation) of crystals similar to those shown in c, soaked in a solution mimicking the natural environment within the bacteria (3) *M* KCl, 0.5 *M* ammonium chloride and 0.05 *M* magnesium chloride). Prior to data collection the crystals were gradually immersed in solution containing the above components and 18% ethyleneglycol for about 30 min, then flash cooled to around 90 K. The patterns were recorded on film (d) or image plate (e) at 85 to 100 K with synchrotron X-ray beam (X11 port at EMBL/DESY). Wave length: 1.488 Å. Exposure times: 7 and 5 min. Crystal to film distance: 330 (d) and 700 mm (e). Resolution at the edge of the patterns: about 4.5 Å.

was found to be essential for obtaining crystals of other particles: B30S, B70S, and T70S(II) (see Table 3).

C. Crystallographic Analysis of Ribosomal Particles

1. The Initial Studies

The diffracting power of crystalline ribosomal particles is so weak that virtually all of our crystallographic studies have been performed with synchrotron radiation.[56] These extremely intense, coherent, and focused X-rays, which are generated as a byproduct of accelerators originally designed for high-energy-particle experiments, are most suitable for crystallographic studies of biological macromolecules.

Even in the early stages when the crystals were extremely small, we could detect a very high degree of internal order in X-ray diffraction experiments of samples containing a large number of microcrystals.[22] As mentioned above, the first diffraction patterns were obtained from microcrystals of 50S subunits from *B. stearothermophilus*, grown from solution containing low-molecular-weight organic solvents in hanging drops. As these microcrystals were extremely sensitive, they could not be handled using the conventional procedures. Consequently, for their crystallographic characterization, they were placed together with their growth medium in quartz X-ray capillaries and paletted by mild centrifugation. The supernatant was then removed and replaced by a fresh one. After several repeats of this procedure there were no indications of ribosomal particles in the supernatant, and the palette was examined by X-rays in a fashion similar to the powder diffraction procedure often used in crystallography of small molecules. The resulting patterns showed fairly sharp rings and oriented arcs with spacing extending to 3.5 Å resolution, resembling the diffraction of partially oriented fibers.[22] Similar spacing were measured previously on diffuse diffraction patterns of gels of *E. coli* ribosomes and of their extracted ribosomal RNA.[57-59]

Crystallographic studies conducted later with large single crystals grown under similar (B50S(I)) or different (B50S(II)) conditions showed similar arcs and rings in addition to the single-crystal diffraction patterns. It is noteworthy that in spite of the fact that the resolution of the well-resolved rotation patterns was around 15 to 25 Å, the oriented arcs were of spacings of much higher resolution limits (up to 3.5 Å), similar to those measured by us on the "powder" patterns and contained also distinct spots.[56] Such patterns may arise from partial orientation of rRNA within the sample. We therefore concluded that some regions, rich in rRNA, within the crystalline ribosomal subunits are of sufficient order on a microcrystalline scale, whereas the disorder the crystal lattice resulted in Bragg diffraction at considerably lower resolution.

2. Mounting Single Crystals in Their Growth Solutions

All crystals of ribosomal particles are extremely sensitive to subtle changes in their environment. An extreme case, mentioned above (Sections II.A.2 and II.B.2.a), is that of the crystals of the 50S subunits from *B. stearothermophilus*, called B50S(I) in Table 3. Since they grew from low-molecular-weight alcohols, which are most volatile, manipulating and handling of these crystals was virtually impossible. Therefore, we chose to grow these crystals directly in X-ray capillaries (Section II.B.2.a and in References 20 and 35 to 38).

Since most of the crystals grew so that one of their faces adhered to the walls of the capillaries, it was possible to irradiate some of them without removing the mother-liquor ("wet mount" in References 36 to 38). Furthermore, although most of the crystals grew with their long axis parallel to the capillary axis, a fair number of them grew in different directions and we were able to find individual crystals in proper orientations for data collection from the three major crystallographic zones without manipulating the crystals. Experiments indicated that crystals kept in their growth media last significantly longer in the X-ray beam and rarely developed as many cracks as those that were partially exposed to air (Figure 5). In general, mounted crystals of biological macromolecules are held at the walls of

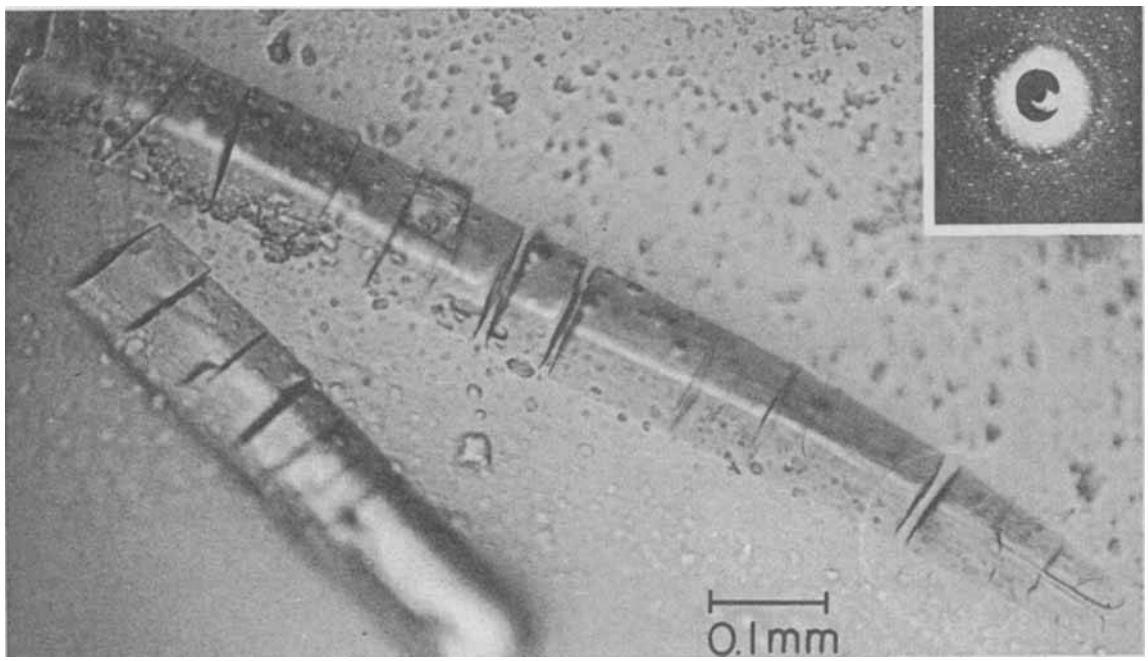

FIGURE 5. A crystal of 50S subunits from *B. stearothermophilus* (B50S(I) in Table 3). The crystal was grown in an X-ray capillary and due to its heavy weight sank to the bottom of the crystallization column (Figure 2) where it was partially exposed to air saturated with vapor of the same composition as that of the crystallization column. As seen the crystal developed cracks perpendicular to its long axis. A "still" diffraction pattern of one of its fragments, obtained with synchrotron X-ray radiation at X11/EMBL/DESY,[35] is inserted.

the capillaries by the surface tension of a small droplet in atmosphere similar to that of the crystallization chamber, which is achieved by the enclosure of small amounts of the stabilization solution at the ends of the sealed capillaries. In our case, despite the better diffraction patterns, the overcrowding of the crystals in the capiliaries hampered data collection. Attempts to reduce the number of crystals grown in each capillary by employing conventional procedures or our special techniques were found to be unsuitable for this system.

3. Cryocrystallography

At ambient temperatures, the radiation damage suffered by crystals of all ribosomal particles is so rapid and so severe that all reflections beyond Bragg spacing of about 18 Å decay within a few minutes, a period shorter than the time required to obtain a single useful X-ray photograph. The extreme sensitivity of the crystals to radiation led us to conclude (incorrectly, as we discovered later) that the diffraction of all our crystal forms was limited to 15 to 18 Å resolution.[35–38] Since diffraction data to higher resolution could be observed only in the first X-ray photograph, obtained from each individual crystal, a new crystal had to be used for each exposure, and precise alignment of the crystals was impossible. In a typical attempt to obtain a complete diffraction data set from crystals of the 50S subunits from *H. marismortui*, (H50S(I)), more than 260 individual crystals were used, but the combination of randomly oriented crystals and short exposures resulted in only partial data sets.

It is generally believed that the damage to biological samples by ionizing radiation is caused mainly by free radicals. These are produced continuously from the first instance of irradiation and can freely diffuse, as crystals of macromolecules include extensive solvent regions. We have been

able to overcome the problem of radiation sensitivity of all the crystals of ribosomal particles by shock freezing of the crystals to cryogenic temperatures (the temperature of liquid nitrogen, about −180°C) before the diffraction experiment, and collecting the crystallographic data at this temperature. We believe that under these conditions the propagation of the free radicals, produced by the interaction between the X-ray beam and the crystalline material is minimized.

For many years, crystallographic data of small organic and inorganic molecules have been collected at cryogenic temperatures. These procedures were developed aiming at obtaining accurate data at very high resolution. During the last 2 decades there have been several attempts to extend this technique to structural studies of biological macromolecules (for review see References 60 and 61). Despite these attempts, the use of cryotemperatures for collecting diffraction data from crystals of biological macromolecules had generally been less successful, mainly due to the assumed need to keep biological crystals in closed X-ray capillaries together with minute amounts of solvent for maintaining a vapor composition similar to that of the stabilization solution. Due to their elongated shape and relatively large size, these capillaries could not be properly shock cooled, and the cooling process caused air drifts, often accompanied by movement of the enclosed crystal or by deposition of microcrystals of the components of the mother liquor within the capillaries. In fact, in only a few cases have such studies been followed to completion.[62]

Our approach was to avoid the X-ray capillaries and to design an experimental procedure that allows a rapid lowering of the temperature of the crystals.[16,40,46,61] For protecting the crystals from drying we have initially employed a procedure, similar to that developed for protecting crystals of air-sensitive or explosive small organic molecules[60] but with some essential modifications. All crystals of ribosomal particles obtained so far are soft, flexible, and easily deformed. When mounted on glass fibers, as is routinely done for crystals of nonbiological compounds or for average-size proteins, they bend around the glass fiber and lose their internal order. Therefore, we constructed a variety of microspatula that allows mounting crystals in desired orientations. Later, a second generation of spatula, made of double layers of thin glass plates ("double-layer" or "sandwich" spatula), was developed.[16,61] These provide extra protection from drying and from bending stresses resulting from surface tension effects. In this procedure, the crystals are immersed in very small amounts of solvents, which, upon cooling, solidify as amorphous materials.

The procedure used for cooling crystals of explosive materials include immersion of the crystals in small amounts of an inert hydrocarbon, which caused dramatic loses of ribosomal crystals due to their hydrophilic nature. To avoid these losses, prior to cooling, the crystals are transferred to solutions that mimic their original stabilizing solutions, but sometimes modified to afford increased viscosity for protection from drying. In some cases it is also necessary to add a cryosolvent,[63] in order to prevent destruction of the crystal by internal ice formation. The choice of the appropriate precooling treatment is largely dictated by the properties of the crystals. A thorough search to establish individual freezing conditions for each crystal form was essential and resulted in our ability to apply the shock-freezing technique to all crystals of ribosomal particles studied by us so far.

It was found that the crystals were cooled best when plunged into an appropriate coolant, such as liquid propane near its solidifying temperature. We constructed an apparatus allowing transfer of the cooled crystals from the propane to the X-ray camera, where they are surrounded by a nitrogen stream at cryotemperature, without being heated or exposed to the atmosphere.[61] The frozen crystals did not show radiation damage over periods longer than needed for collecting complete diffraction data sets (days or even weeks). Furthermore, we have constructed a device for preserving irradiated crystals in solid propane that enabled us to resume interrupted diffraction experiments at a later date. To assess the influence of the cooling and the storage on the quality of the results, we compared the diffraction data of a crystal at the beginning of data collection with that collected after irradiation of 48 h and after 153 d of storage in solid propane. In no case could we observe any significant loss of diffraction.

A quantitative assessment of the effect of the cooling on the properties of the resulting diffraction patterns, such as the resolution and the mosaic spread is still impossible, mainly because the same crystal cannot be exposed both at room and cryotemperatures due to the irreversibility of the effects of radiation damage. On the other hand, a comparison between data collected from different crystals may be misleading due to the considerable heterogeneity among individual crystals, even when grown and examined under the same conditions (Figure 6). However, since the recently grown crystals of form H50S(I,Cd) appear to be rather homogenous, we anticipate more information in due course.

The resolution limits of the diffraction patterns measured at cryotemperatures are not higher than those obtained at ambient temperatures, since these limits originate from conformational heterogeneity, which is not improved by cooling. On the contrary, it appears that the various steps in the cooling procedure, with their associated thermal, osmotic and mechanical stresses, may lead to a partial deterioration of crystal order. However, since at cryotemperature the crystals can be irradiated for a long time, the higher resolution reflections, which are usually very weak, could be detected. Thus, an apparent improvement in the distribution of crystals that show a high potential resolution (see below, Section II.C.4) was observed (Figure 6). In general, the mosaic spread of the diffraction data appeared similar at room and cryotemperatures and it is still premature to determine if there is a systematic small difference in mosaicity between cooled and uncooled crystals. Our experience is also too limited to permit a thorough comparison of data collected at cryotemperature under different cooling conditions. Neither can we currently address the intriguing question of how the cooling influences the resulting structure. Although it remains to be seen whether data collected from our crystals at cryotemperature have the potential to yield an interpretable electron density map, it is of

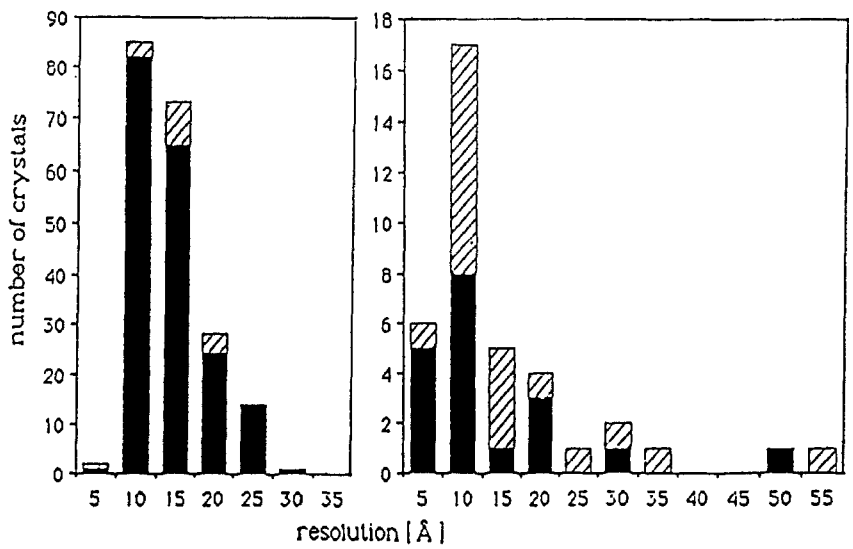

FIGURE 6. The effect of the cryogenic treatment on the ability to detect the highest potential resolution, as measured for crystals of 50S subunits from *H. marismortui* (H50S(I)). The distribution of the approximate best resolution (a) of the first exposure of each of about 230 crystals exposed to synchrotron radiation (station X11, EMBL/DESY) at 4 to 9°C and (b) of about 85 crystals exposed to X-rays at cryotemperature (at EMBL, CHESS, and SSRL). Precooling conditions: gradual immersion in 18% ethyleneglycol for 15 to 60 min prior to freezing in liquid propane at 90 to 93 K. Note the higher fraction of crystals diffracting to 5 to 10 Å.

course our hope that they do contain the key to the determination of the three-dimensional structure of ribosomes.

4. Potential and Usable Resolution

The column "resolution" in Table 2 shows values between 3 and 20 Å, depending on the source. It refers to the highest resolution for which sharp diffraction spots could be observed consistently. We named this value the "potential" resolution, since in many instances we could not collect useful crystallographic data to this resolution. As there is considerable variability in the potential as well as in the useful resolution of the diffraction data obtained from different crystals, even among crystals from the same batch (Figure 6), we believe that the current best resolution is only a temporary upper limit. This is particularly true for the crystals of the 50S subunit from *H. marismortui* (form H50S(I), which diffract to a rather high resolution, 4.5 Å. These crystals are thin plates that are evidently very susceptible to the mechanical stresses of shock cooling. Hence, we anticipate that the intrinsic order of the crystals is better than the current resolution limits.

Other crystal forms for which we expect to obtain higher resolution are those of complexes of ribosomes with selected distinct components of the protein biosynthesis (see below, Section V.B and in Reference 45). We also hope to find the crystallization conditions under which the microcrystalline order, which gives rise to the high-resolution sharp arcs in the patterns of the 50S subunits from *B. stearothermophilus* (see above, Sections II.C.1 and 2 and in References 22 and 56), will be extended to the entire crystal.

III. ATTEMPTS AT PHASING

Determination of the three-dimensional structure of a crystalline compound by X-ray crystallography involves a Fourier summation of the reflections present in its diffraction pattern. Each reflection is a wave characterized by its direction, intensity, and phase. The direction and amplitude of a reflection can be measured, whereas the phase cannot be directly determined. For macromolecular crystals, two methods are commonly used to determine phases: the multiple isomorphous replacement (MIR) and the molecular replacement methods.

A. MIR: Specific and Quantitative Labeling of Ribosomal Particles Using Dense Multimetal Clusters

Phase determination by MIR involves the preparation of at least two derivatives of the unknown molecule, usually by the introduction of one or a few electron-dense atoms or groups of atoms to the crystalline lattice at distinct locations. The added atoms, or groups of atoms, should be dense enough to cause measurable changes in the diffraction pattern of the unknown molecule, while keeping the crystal structure isomorphous to that of the native molecule. If these conditions are met and the number of added groups is small, their locations can usually be deduced from maps constructed from differences of intensities between the diffraction pattern of the native crystal and of its heavy-atom derivative (called "Patterson difference maps").

For proteins of average size (e.g., with molecular weights of 15 to 80 kDa), a useful isomorphous derivative consists of one or two heavy-metal atoms. Due to the large size of the ribosome, an ideal compound to be used for its derivatization should consist of a compact cluster of a proportionally larger number of heavy atoms linked directly to each other. Two such clusters, an undecagold cluster (GC), with a total molecular weight of 6200 Da and a tetrairidium cluster (IC), with a molecular weight of 2300 Da have been synthesized.[64–66] Although never used before for this purpose, we have designed monofunctional reagents of the two clusters to facilitate specific derivatization of the ribosomal particles or of compounds with a high affinity to the ribosomes by covalent binding of these clusters.

According to Crick and Magdoff,[67] if one assumes full occupancy of the gold cluster in one site on each of the 30S, 50S, and 70S particles, the average change in diffraction intensities is expected to be about 19, 15, and 11%, respectively. Hence, provided these requirements are fulfilled, the undecagold cluster is likely to induce measurable differences between the intensities of the reflections of the native crystals and those of the derivatized one that may lead to phase information. As the core of the undecagold cluster is about 8.2 Å in diameter,[64,65] it can be treated as a single scattering group at low to medium resolution. The tetrairidium cluster has a core diameter of about 5 Å,[66] and can thus be treated as a single heavy atom to somewhat higher resolution.

Derivatives of crystals of biological macromolecules are routinely obtained by soaking crystals in solutions of the heavy-atom compounds or by cocrystallization of the macromolecule together with the heavy atom. Using this procedure, the number of heavy atoms that bind to the macromolecule is largely a matter of chance, but the chances of obtaining a useful derivative for a typical macromolecule with these equilibrium techniques are sufficiently high so that more sophisticated techniques are rarely needed. However, since ribosomal particles have an extremely large and complex surface area, it would clearly be preferable not to leave the binding of the heavy atom to pure chance. An alternative procedure for derivatization is covalent binding of the heavy atom compound to the molecule at a specific site before crystallization. This approach requires sophisticated synthetic techniques and time-consuming purification procedures, but it offers a much better chance of obtaining a unique derivative. Specific derivatization of selected ribosomal components may have a considerable value not only in phasing the crystallographic data, but also in localization of specific sites on the ribosomes, information that may be indispensable for the understanding of the function of the ribosome.

To facilitate quantitative binding of heavy-metal clusters to specific active moieties on the surface of the ribosome, the clusters were prepared as monofunctional reagents.[32] The first targets for binding the clusters were the free sulfhydryls on the surface of the particles, which were detected by their reactions with radioactive markers, such as *N*-ethyl-maleimido (NEM), parachloromercurobenzoate (PCMB), and iodoacetamide, followed by polyacrylamide gel electrophoresis of the ribosomal proteins. Those proteins that had reacted with the markers were identified by the radioactivity of their corresponding spots. We were able to define conditions for minimizing the number of exposed sulfhydryl groups, and to bind (at different yields) the cluster to 1 to 3 sulfhydryls on the surface of each ribosomal particle that is being studied by us so far (Table 1).

Since the gold cluster is rather bulky, its accessibility was enhanced by attaching to it a maleimido group through aliphatic chains of varying lengths. The $-SH$ groups on the surface of the 50S particle were also extended in a similar manner. Radioactive labeling of the gold cluster, as well as neutron activation analysis of both the gold and the iridium clusters, enabled us to determine the extent of binding of these clusters to the particles. The results of both analytical methods show that a spacer of a minimum length of about 18 Å between the $-SH$ group on the ribosomal surface and the N-atom of the cluster is needed to allow efficient binding of the gold cluster directly to the 50S particle.[13,17,32,41-43] An almost quantitative binding of the cluster to a single site on the 70S ribosome and on the 30S subunit from *T. thermophilus* could be achieved, and the modified particles yielded crystals that are smaller than but isomorphous with the native ones. High-quality crystallographic data could be collected from both forms. We were also able to bind the clusters at a rather low yield (35 to 65%) to one and to two sites on the surfaces of 50S subunits form *H. marismortui* and *B. stearothermophilus*, respectively.[13]

A more elegant and innovative procedure for obtaining a defined heavy atom derivative was based on the development of a mutant of *B. stearothermophilus*.[31] In this mutant one ribosomal protein, BL11, is omitted. The mutated 70S ribosomes and 50S subunits formed three-dimensional crystals and two-dimensional sheets isomorphous to those of the respective wild-type particles.[13,17,28,32,38,40-43] Thus, we concluded that the absence of BL11 did not cause gross conformational changes in the ribosomal particles,

and that it is not crucial for the interparticle interactions forming the crystallographic network. Similar attempts to grow crystals of ribosomal particles depleted of protein BL12 failed, either because the absence of BL12 influences the overall structure of the particle, as has been observed for 50S ribosomal subunits from *E. coli*,[68] or because BL12 is involved in the interparticle crystalline network.

Conditions for gradual detachment of a few selected proteins from the ribosomes of *B. stearothermophilus* and their consequent reconstitution into the core particles were determined.[69] One of the detached group of proteins, BL11, could be chemically modified prior to its reconstitution. It is noteworthy that protein BL11 is an example of a ribosomal component that undergoes reversible conformational changes upon isolation from the particle. When incorporated in the ribosome, its single free $-SH$ group is exposed and chemically reactive. In isolation, however, this group is not reactive unless the protein is denatured. The gold and the iridium clusters could be quantitatively bound to isolated BL11 under denaturing conditions, and the denatured modified protein refolds to its regular *in situ* conformation when incorporated into the mutated ribosomal core, leading to the formation of specific and quantitatively modified particles, which are biologically active even though the large heavy-atom cluster is attached to them.[32] To place the size of the clusters into perspective, we note that the molecular weight of the undecagold cluster (6200 Da) is more than a third of the molecular weight of BL11 (15,500 Da).

Both two-dimensional sheets and three-dimensional crystals, isomorphous with the crystals of the native particles, could be obtained from 50S subunits reconstituted with covalently labeled BL11 under the same conditions used for the crystallization of the native particles (Figure 7 and in References 13 and 32). X-ray diffraction data, of a quality comparable to that obtained from the native crystals, were collected from crystals of the modified particles and Patterson maps, constructed from the differences in the intensities between the derivatized and the native crystals included features that could be interpreted. These experiments demonstrate that it is possible to label ribosomes by specific covalent binding of heavy-atom clusters without introducing major changes in their crystallizability, integrity, or biological activity. Thus the attachment of heavy-atom clusters to isolated ribosomal components, followed by reconstitution of the modified component into ribosomal particles, should provide a tool for obtaining heavy-atom derivatives useful for phase determination.

Attempts to apply a similar approach to halophilic ribosomes have met with considerable difficulties. Quantitative removal of specific ribosomal proteins from eubacterial sources can be achieved by stepwise addition of salts, sometimes together with alcohols, to their storage buffers, under well-defined conditions.[69] In the case of the halophilic ribosomes, the natural salinity required to maintain their integrity and activity is so high that a substantial addition of salts together with organic materials is not possible. The obvious approach would be to attempt to split off halophilic ribosomal proteins by decreasing the salt concentration. Indeed, a total removal and reconstitution of the ribosomal proteins of several halophilic bacteria was achieved in this manner,[70] but this protocol does not appear to be suitable for selective dissociation of small numbers of proteins. Therefore, an alternative procedure, based on the addition of organic solvents, had to be established.

Dioxane was found to be a suitable chemical agent for partial removal of several proteins from ribosomes of *H. marismortui*, all of which could be quantitatively reconstituted into the core particle. One of the removed proteins, tentatively named HL11, can bind reagents specific to $-SH$ groups, such as NEM or the gold cluster, but the modified protein could not be incorporated into the core particle. However, since in this way protein HL11 can be quantitatively removed from 50S subunits under very mild conditions, it might prove useful, in the course of structure determination, to relate to native 50S subunits as $+HL11$ derivatives of the HL11-depleted core particles.

The results of these experiments, as well as of our attempts to mutate the halophilic ribo-

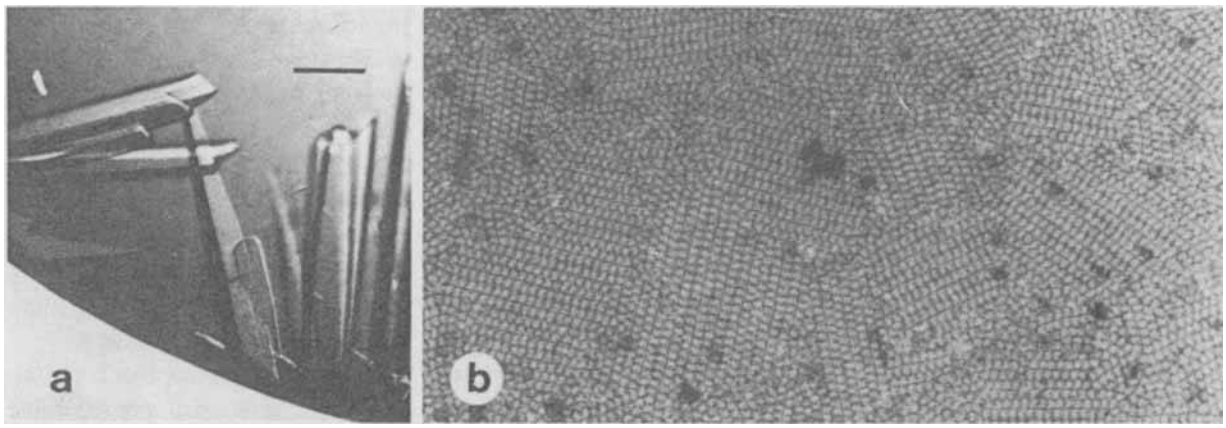

FIGURE 7. (a) Three-dimensional crystals and (b) two-dimensional sheets of 50S subunits from *B. stearothermophilus* derivatized with the undecagold cluster,[32,64,65] by reconstitution of protein BL11 to which the cluster was previously covalently bound, into core particles of mutated ribosomes (mutant TST (31), lacking protein L11). Growth conditions for a as for B50S(GC) in Table 3, and for b as in Reference 44. (Bar = 0.2 mm.)

somes, pose interesting questions as to the role of protein HL11 and its interactions with other components of the ribosome. These interactions are clearly weaker than those of the other ribosomal proteins, as it is the only protein of ribosomes from *H. marismortui* that can be selectively dissociated.

A potential approach for obtaining a suitable heavy-atom derivative of these particles is the exchange of a selected ribosomal protein, which does not possess an exposed −SH group with its homolog from another bacterial source, that contains such moiety. In a preliminary step using this approach, protein L12 from the ribosome of *methanococal vannielii* could be incorporated into core particles obtained by depleting ribosomes of *H. marismortui* of the homologous protein.[71] An extension of these ideas is the genetic insertion of cysteines to selected sites on the surface area of the ribosome.[117]

An obvious target for indirect attachment of heavy-atom clusters to ribosomal particles is tRNA. To facilitate cocrystallization of tRNA with ribosomal particles, we have determined conditions for stoichiometric binding of tRNA to several ribosomal particles. One of the resulting complexes mimics a defined state in the process of protein biosynthesis is composed of the whole 70S ribosome, a short segment of mRNA, and two molecules of charged tRNA (See Section V.B and Reference 45). In fact, any compound that forms a tight, specific complex with ribosomal particles can in principle be used as a carrier for the heavy-atom clusters. In addition to the tRNA molecule, appropriate candidates may be mRNA, antibiotics,[72] or DNA oligomers complementary to exposed single-stranded rRNA regions.[73,74] Since most of the interactions of such carriers are well characterized biochemically, crystallographic location of the heavy-atom clusters attached to such compounds should provide information useful not only for phase determination but also for the localization of structural and functional sites on the ribosome.

B. The Molecular Replacement Method

Because ribosomal particles are much larger than any macromolecular complex solved by X-ray crystallography to date, one can anticipate that it will be difficult to fulfill all of the requirements of an ideal isomorphous derivative simultaneously. Therefore, we are pursuing a strategy that combines elements of both the molecular replacement and the MIR methods.

When an approximate model for an unknown crystalline macromolecule is available, or the unknown macromolecule is closely related to one whose structure is known, the model or the known structure may provide preliminary phase information for the unknown one. This approach to

phase determination is known as the molecular replacement method. It is based on the positioning of the known model in the unit cell of the unknown structure.

We have derived low-resolution, three-dimensional models of 70S ribosomes and 50S ribosomal subunits of *B. stearothermophilus* by image reconstruction using electron-microscopy diffraction data from tilt series of two-dimensional arrays of these particles (see below, Section IV.A.2 and in References 75 to 78). These low-resolution models are currently being used for molecular replacement searches together with the crystallographic data from crystals of 70S ribosomes from *T. thermophilus* and 50S ribosomal subunits from *H. marismortui*. The use of reconstructed images of ribosomal particles of one bacterium with data obtained from crystals of ribosomal particles from other prokaryotic sources is based on the assumption that the gross structural features of ribosomes from different bacterial sources are similar at the low resolution (28 to 50 Å) used for the reconstruction. For convenience, the reconstructed models were represented as pseudo-macromolecules, which consist of an envelope or a boundary filled with a large number of group scatterers, each representing several nonhydrogen atoms (see below, Section IV.A and in Reference 33). These group scatterers were initially positioned on the grid points of the reconstructed density map at values higher than a set threshold. To avoid unrealistic regularity in the positions of the pseudo-atoms, the coordinates of the group scatterers were randomized using a distribution random number generator.[33]

C. *In situ* Complexes

The knowledge of the accurate structures of individual ribosomal components may be of instrumental assistance in the determination of the structure of ribosomes using the molecular replacement method. Despite extensive efforts, so far only a small number of isolated ribosomal components could be crystallized, and only a few of them have been subjected to crystallographic analysis that matured in a detailed molecular structure.[69,79–87] This may indicate that the internal interactions contribute significantly to the stabilization of the conformation of the individual components within the assembled ribosome and explain why several ribosomal components loose their *in situ* conformation when they are detached from their supporting environment. At the same time it is anticipated that provided the association with the *in situ* closest neighbors is maintained, isolated internal ribosomal complexes are likely to keep their natural conformations in solution. Assuming crystallization and structure determination they should yield valuable structural and phase information.

We have begun to purify complexes of ribosomal components with a defined RNA/protein composition, high stability, and relatively low molecular weights. The first one, of HL1 with 23S RNA (from *H. marismortui*), has been isolated and characterized.[119]

IV. SUPPORTING DIFFRACTION TECHNIQUES

The determination of the structures of biological macromolecules hinges on merging the crystallographic results with other relevant information. For the particular case of the ribosome, besides the instructive interplay with the functional, biochemical, and biophysical studies (see below, Section V), we found that it is essential to complement and support our crystallographic work by other diffraction techniques. These include neutron diffraction from three-dimensional crystals, image reconstruction from tilt series of electron-micrographs of two-dimensional sheets, and electron-microscopical investigations of thin sections of embedded three-dimensional crystals. Although the X-ray diffraction patterns extend to a higher resolution than at present one can reasonably expect to obtain with either of the other diffraction techniques, the strengths of these methods lie in their ability to provide approximate models in the absence of heavy-atom derivatives. It is likely that these low-resolution models will be useful, if not crucial, for the X-ray structure determination.

A. Electron Microscopy

The large size of the ribosome permits its investigation by electron microscopy at various stages of the crystallographic work. We first used the electron microscope as a diagnostic tool for directing us in the choice of crystallizable ribosomal particles. It enabled us to follow the initial steps of crystal growth and to detect the formation of crystalline material too small to be seen otherwise (Figure 3). In this way we could rather rapidly assess the tendency to crystallize of several native and modified ribosomal particles, in contrast to the time needed for the detection of visible crystals. This allowed us to establish favorable conditions for the growth of well-ordered crystals. In later stages, images of positively stained thin sections of embedded three-dimensional crystals provided important information on the quality of these crystals and on their packing motifs. In some cases, thin sections could also be used for three-dimensional image reconstruction aimed at the gross location of different chemical components at low resolution (see Section IV.A.1).

1. Electron Microscopy of Sectioned Three-Dimensional Crystals

In the early stages of our studies, we were able to obtain micro three-dimensional crystals that were too small for single-crystal X-ray or neutron crystallography, but at the same time, too thick for direct investigation by electron microscopy. Therefore, we used thin sections of these crystals for investigating their internal packing arrangements. These sections were sliced from cross-linked epon-embedded crystals and then positively stained with uranyl acetate or similar compounds. For some of the crystal forms, those that are still not suitable for single-crystal X-ray crystallography, such as the microcrystals of the 70S ribosome from *E. coli* (Figure 8 and in References 29, 30, and 37), this was the only feasible approach. For the other crystal forms, which eventually reached sizes suitable for crystallographic studies, the information (Figure 9) from the electron microscopical studies is currently being used for extracting initial information about their packing motifs.

In rare cases, under favorable experimental conditions, positively stained thin sections may also be used for image reconstruction studies. Such analysis is limited by the inherent lower resolution of the sectioned material, by the uncertainty regarding the exact sectioning direction, and by the still unknown factors governing the stain distribution within the particle. However, despite these shortcomings, there are some important merits to such studies, and they were performed on the four crystal forms of 50S subunits from *B. stearothermophilus* (Figure 10 and in References 37 and 88). As mentioned above, the sections used for these studies were obtained from cross-linked and epon embedded crystals, a treatment that enhances the stability in the electron beam. Therefore, up to 92 tilted images could be obtained from a single sample (23 images around four different tilt axes). The diffraction patterns of these images were merged together and produced rather reliable stain-distribution maps.

Although packed differently, all the reconstructed models showed essentially the same stain distribution within the particle.[88] They consist of two domains of unevenly distributed density (Figure 10), which may originate from preferential staining of selected parts of the particle. These models are in good accord with the results of the three-dimensional image reconstruction from two-dimensional sheets,[75,78] obtained a few years later at significantly higher resolution from samples grown under different crystallization conditions and exposed to completely different experimental treatments (Figures 11b, 12a and b, 13 a to c).

Besides the information about the packing modes of the crystalline ribosomes and about their overall structures, the thin sections were also used for investigating the distribution of the different chemical entities within the ribosomal particles. We preferentially aimed to stain the ribosomal RNA, taking advantage of its rather high affinity to the commonly used stain, uranyl acetate. In parallel, regions rich in ribosomal proteins could be identified, although not as clearly, by staining with phosphotungstic acid (PTA). The results of these studies were in accord with those obtained from unstained, naturally formed two-dimensional sheets of ribosomes from oocyte of liz-

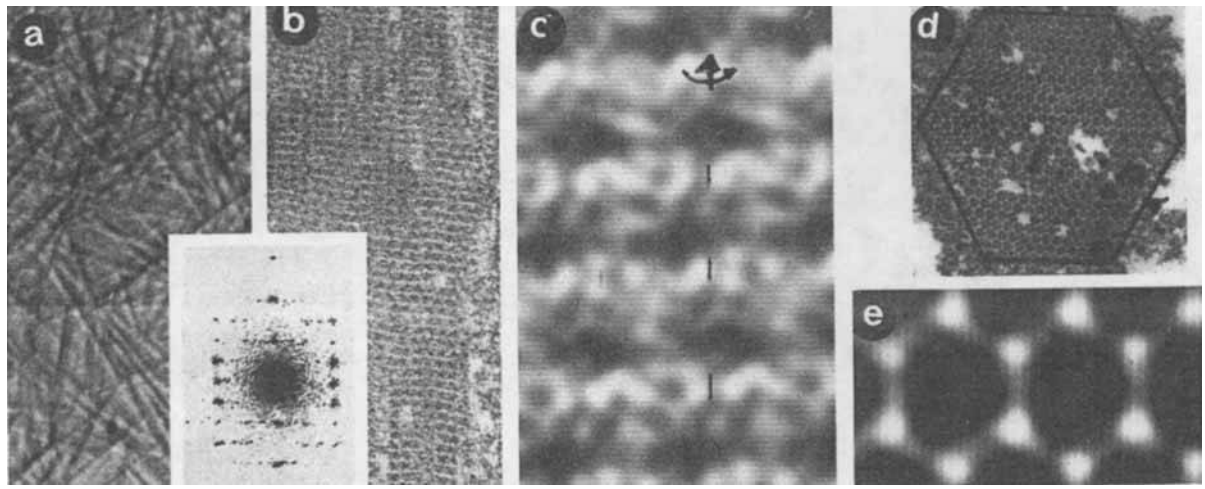

FIGURE 8. Results of electron microscopy of positively stained thin sections of epon-embedded microcrystals of 70S ribosomes from *E. coli*. (a) Microcrystals grown as in Reference 29, b and d are sections perpendicular to the long crystal axis, c and e are filtered images of the sections shown in b and d respectively. The boundaries of the crystals are depicted on d. An optical diffraction pattern of b, which shows a 2_1 (or 6_3) screw axis, is inserted. The approximate direction of this axis is marked on c.

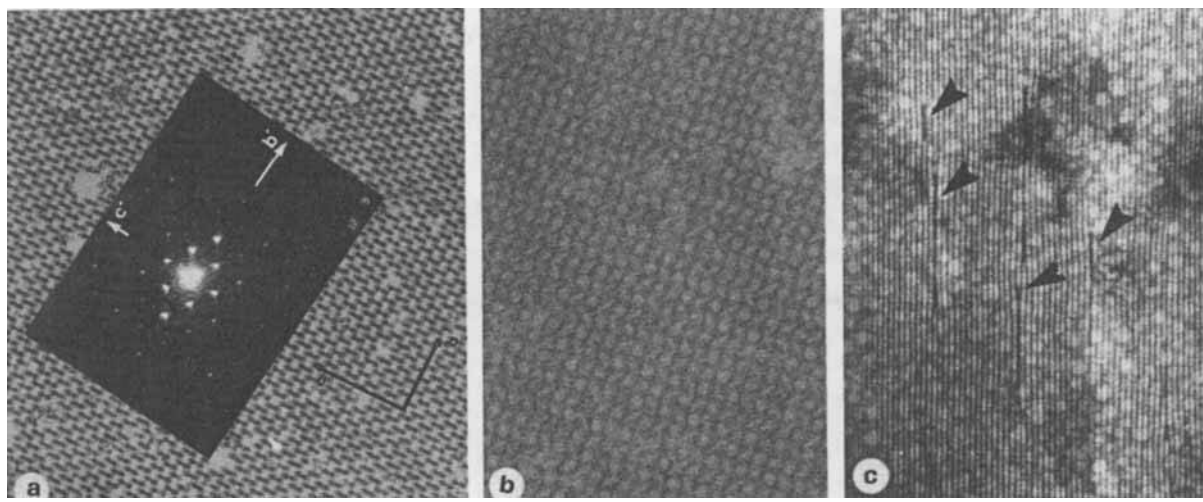

FIGURE 9. Positively stained thin sections of epon-embedded crystals of (a) 50S subunits from *B. stearothermophilus* (B50S(I) in Table 3), (b) 30S subunits of *T. thermophilus* (T30S in Table 3), and (c) 70S ribosomes from *T. thermophilus* (T70S(I) in Table 3). The optical diffraction of a, which could be correlated with the X-ray diffraction patterns of this crystal form[37] is inserted. In b the fourfold axis is evident; in c the locations of defects in the crystal are marked. These or similar ones may be the reasons for the high mosaic spread observed for this crystal form. Note that the crystal "repairs" itself.

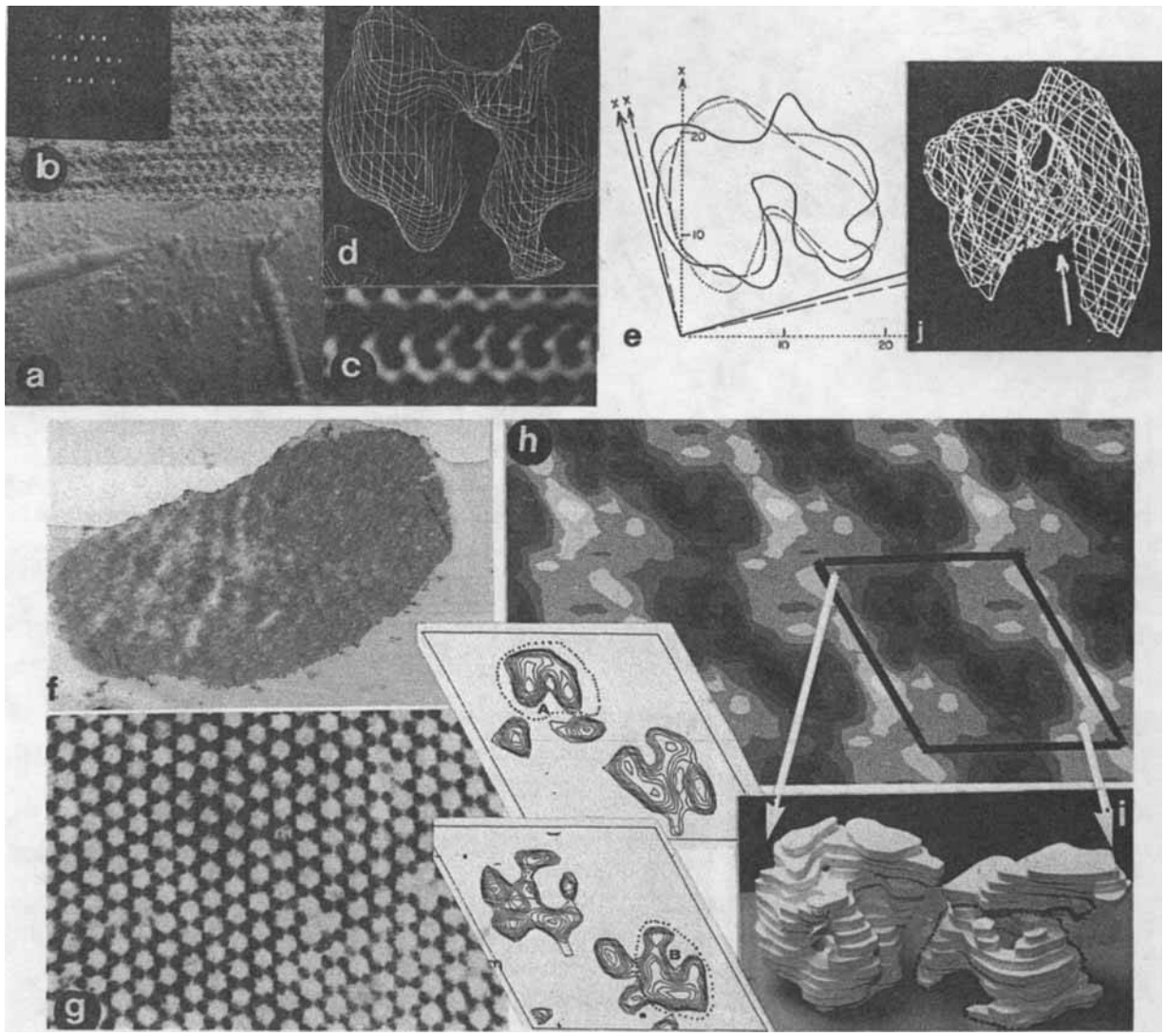

FIGURE 10. Attempts in three-dimensional image reconstructions of large ribosomal subunits from *B. stearothermophilus* using positively stained thin sections of B50S(I) in Table 3. (a) Crystals, from form #1 in Reference 88; (b) a thin section of an embedded crystal similar to those shown in a, positively stained with uranyl acetate. Insert: its diffraction pattern; (c) the filtered image of b; (d) the reconstructed stain density from two perpendicular tilt series of b. (e) a superposition of the reconstructed images of forms #1, #2, and #3;[88] (f) shows a section through a whole crystal, called #4 in Reference 88; (g) an enlarged part of f; (h) the filtered image of g in which the asymmetric unit, believed to contain four 50S subunits, is delineated; (i) a physical model of the reconstructed asymmetric unit shown in h using two perpendicular tilt series of positively stained thin sections of a crystal similar to that shown in f. Depicted is the assumed single 50S subunit. Note that more than one particle is shown. Inserted are two sections of the stain-density map of the area depicted in h, 60 Å apart, along the perpendicular axis. Note the similarity between (j) the reconstructed image from the negatively stained two-dimensional sheets (at medium resolution, 28 Å) and that of the stain distribution shown in d, e, i, and the inserted sections of the density map.

ards,[9] as well as from the contrast variation in neutron scattering studies of *E. coli* ribosomes.[89] All showed that rRNA-rich regions are concentrated in the interior of the ribosomes as well as at the interface area between the large and small subunits.

2. Image Reconstruction from Periodically Ordered Two-Dimensional Arrays

We used electron micrographs of tilt series of two-dimensional sheets to reconstitute three-

dimensional models for ribosomal particles. These are currently being used in attempts to phase the X-ray crystallographic data at low resolution.

For over 3 decades a considerable effort was dedicated to direct visualization of single ribosomal particles by electron microscopy. Several limitations are common in electron microscopy of biological specimens. These arise from the difficulties of preserving biological materials in the vacuum of the microscope from uncontrolled shrinkage, probable collapse of the structures on the flat grids, radiation damage, complications introduced to the interpretation of images obtained by the staining procedures because the information obtained from negatively stained particles actually shows regions of stain rejection, and from uncertainties in choosing the contour level that defines the envelope of the imaged particle. Despite the inherent limitations of electron microscopy, it has provided valuable structural information, especially when coupled with immunological techniques. In this approach, antibodies, specific for antigenic components of isolated ribosomal proteins, were bound to the surface of the assembled particles to reveal, within the limitations of the dimensions of the antibodies, the possible relative locations of the antigenic determinants.[1,2,90]

Our approach was to conduct diffraction studies using periodically ordered monolayers (also called two-dimensional sheets or arrays) of ribosomal particles for the reconstruction of three-dimensional images. These systems are not free of the limitations listed above, but at the same time the study of ordered arrays differs fundamentally from investigating single particles. Image reconstruction from such an array is inherently more objective, as it is based on diffraction data, whereas single-particle techniques involve averaging of selected particles chosen by statistical or visual correlations that often involves significant subjective judgment. Moreover, the contacts of the dispersed single particles with the microscope grid may introduce severe structural distortion, whereas two-dimensional crystals are less affected by the interactions with the grid, as the crystallized particles are held and supported by lattice forces. Distortions that might be introduced by the electron microscopic grids are thus reduced or even completely eliminated.

Unexpectedly, in contrast to the relative ease in defining the conditions for the growth of three-dimensional crystals of ribosomal particles, many difficulties have been encountered in our attempts to produce two-dimensional crystalline sheets. The first growth of two-dimensional arrays was reported more than a decade ago by Lake. These arrays were of 50S subunits from *E. coli*,[91] obtained over periods of weeks or even months and yielded diffraction information that was only marginally suitable for image reconstruction studies. Thus, the resulting reconstructions had limited resolution and showed little detail.[92,93] Similar albeit larger arrays were grown a few years later in our laboratories from 50S subunits from *B. stearothermophilus*[53] by employing essentially the same crystallization conditions used for the production of the three-dimensional crystals from the same source (form B50S(I) in Table 3) but varying the relative concentrations of the materials in the crystallizing medium, i.e., lowering the concentration of the subunits and increasing the Mg^{2+} concentration.[53] These sheets yielded a preliminary three-dimensional model for the 50S particles at 32 Å resolution.

More recently we developed a procedure for growing well-ordered sheets of ribosomal particles (Figure 11) within a few seconds using combinations of salts and alcohols as crystallizing agents[75–77,94] Ammonium sulfate together with minute amounts of ethanol were used for the production of two-dimensional sheets of 50S and 70S particles from *B. stearothermophilus*. tilt series of well-ordered arrays, negatively stained with gold thioglucose, were used for the image reconstructions and yielded approximate models for these particles (Figures 12, 13, and in References 75, 77, and 78). In some projections (e.g., those shown in Figures 11a and b) our models resemble the images seen when single ribosomal particles are visualized by electron microscopy (for review see References 1, 2, and 90). However, there are some discrepancies between our models and the others, which may stem from the basic differences between the subjective visualization of isolated particles in projection and the inherently more objective character of structure analysis by diffraction methods.

It is noteworthy that the ribosomes from *T. thermophilus*, which yield quality three-dimen-

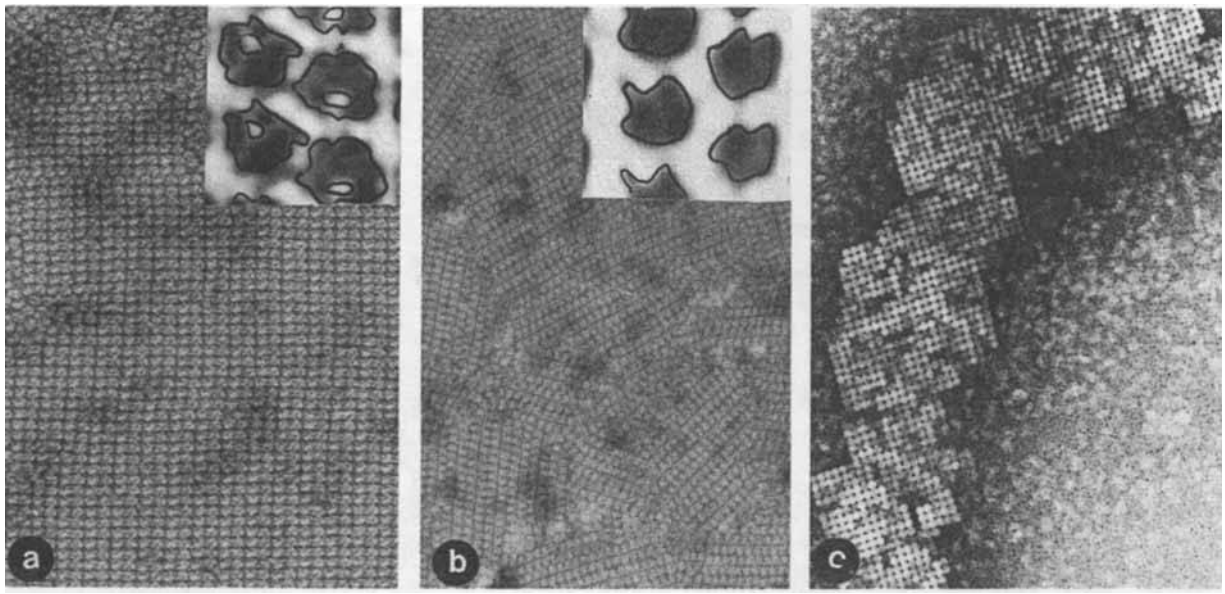

FIGURE 11. Two-dimensional sheets of (a) 70S ribosomes and (b) 50S ribosomal subunits from *B. stearothermophilus*; (c) 30S subunits from *T. thermophilus*. Inserted are filtered images of the corresponding sheets.

sional crystals of 30S, 50S, and 70S particles as well as of several isolated ribosomal proteins (see above, Sections II.B.2.b and III.C), were not useful for the production of periodically ordered monolayers. However, very thin laminar microcrystals of 70S ribosomes of this bacterium obtained from solution containing MPD in the presence[95] or absence of KCl[121] could be placed on the electron microscope grids and partially dissolved to produce thin layers of poorly defined thickness. "Pseudo" monolayers obtained in this way were found to be potentially useful in structural analysis at low resolution.[122]

The advantages of three-dimensional image reconstruction from tilt series of ordered two-dimensional sheets is demonstrated by a comparison of the results obtained in independent reconstructions of whole ribosomes from chick embryo[10] or *B. stearothermophilus*,[77,78] and from 50S ribosomal subunits from the latter.[75] In all three cases, despite the low resolution of the reconstructed images (55, 47, and 28 Å, respectively), these models showed several key features mainly associated with internal vacant spaces or partially filled hollows, which had not been detected by earlier electron microscopic studies. Furthermore, despite some variations in the details of the reconstructed images of the 70S ribosomes and the 50S subunits, both from *B. stearothermophilus*, it was found that there are significant similarities in the overall shapes and in several specific features of corresponding regions of the different models, especially when the 50S reconstruction is examined at a resolution similar to that of the model of the whole ribosome (i.e., around 50 Å). Thus, it was possible to use these similarities to assess the reliability of the models, to locate the 50S subunit within the 70S ribosome, to suggest a model for the associated 30S subunit, and to tentatively assign biological functions to several structural features (Figure 13 and in References 13, 17, and 78).

Despite the advantages of image reconstruction from ordered sheets, the models so obtained suffer from several uncertainties inherent in the method. Besides the shortcomings listed above (e.g., shrinkage of the samples), another source of uncertainty in the shape and the size of the reconstructed particles originates from the limited order of the two-dimensional sheets. Being monolayers, their periodicity is expressed in only two dimensions, hence the structural elements along the lengths and the widths of the sheets can be directly determined, whereas the structure along the vector perpendicular to the sheet (normally designated the c axis) must be derived from indirect information. When placed on an electron microscope grid the sample can be visualized only in projection, and the contribution of the third dimension to the diffraction pattern must be

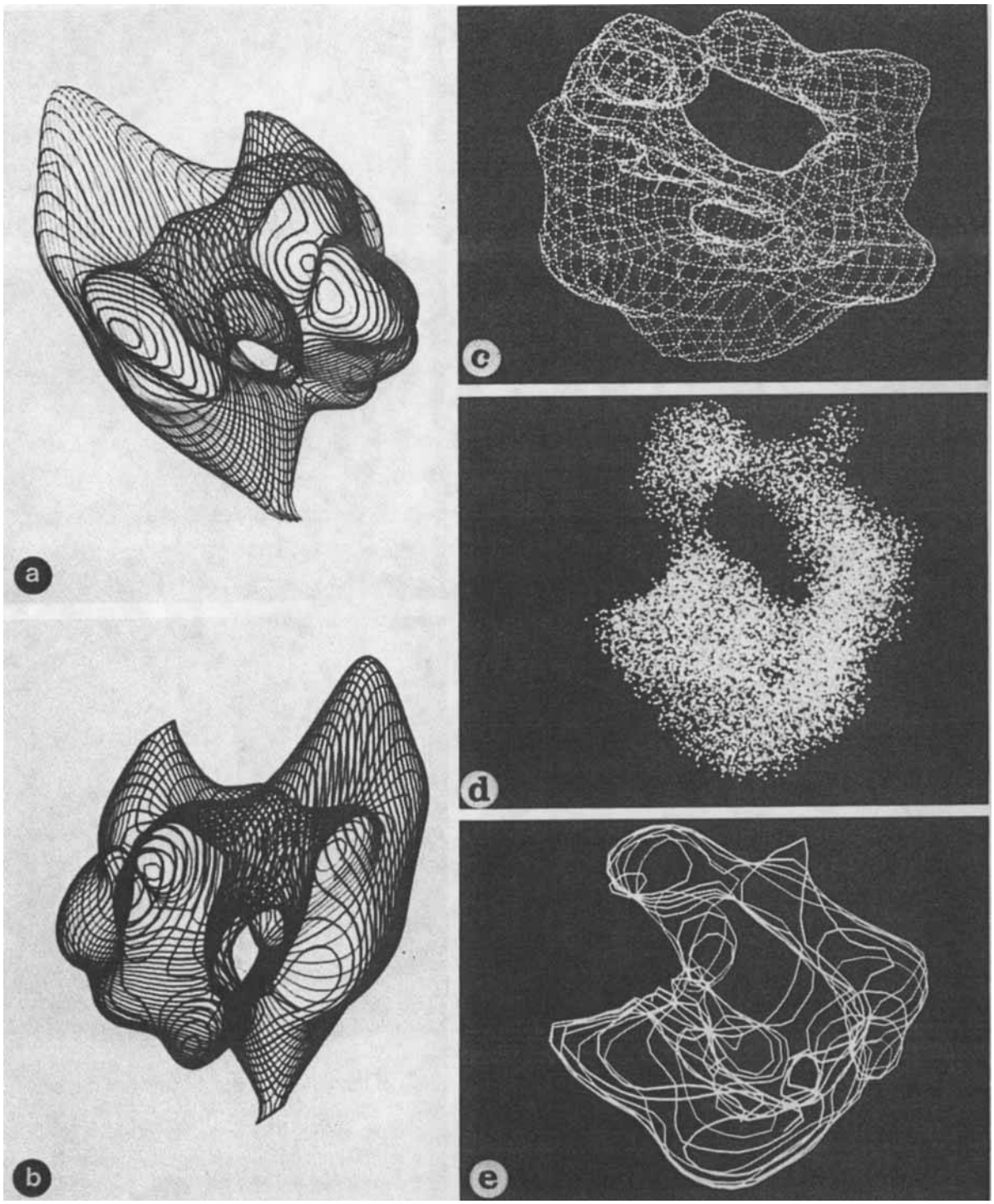

FIGURE 12. Three different representations of the envelopes of the reconstructed models of the 70S ribosome and its large subunit. (a, b) Two views of the reconstructed model of the 50S ribosomal subunit displayed in fine lines, showing clearly the exit of the tunnel and (c to e) three views of the two typical models of the 70S ribosome, represented as a net, pseudo atoms, and in lines, all showing the intersubunit space and the entrance into the tunnel. (c and d or e) are the results of different reconstructions. The representation in d is by 8900 group-scatterers, each representing about 15 nonhydrogen atoms.

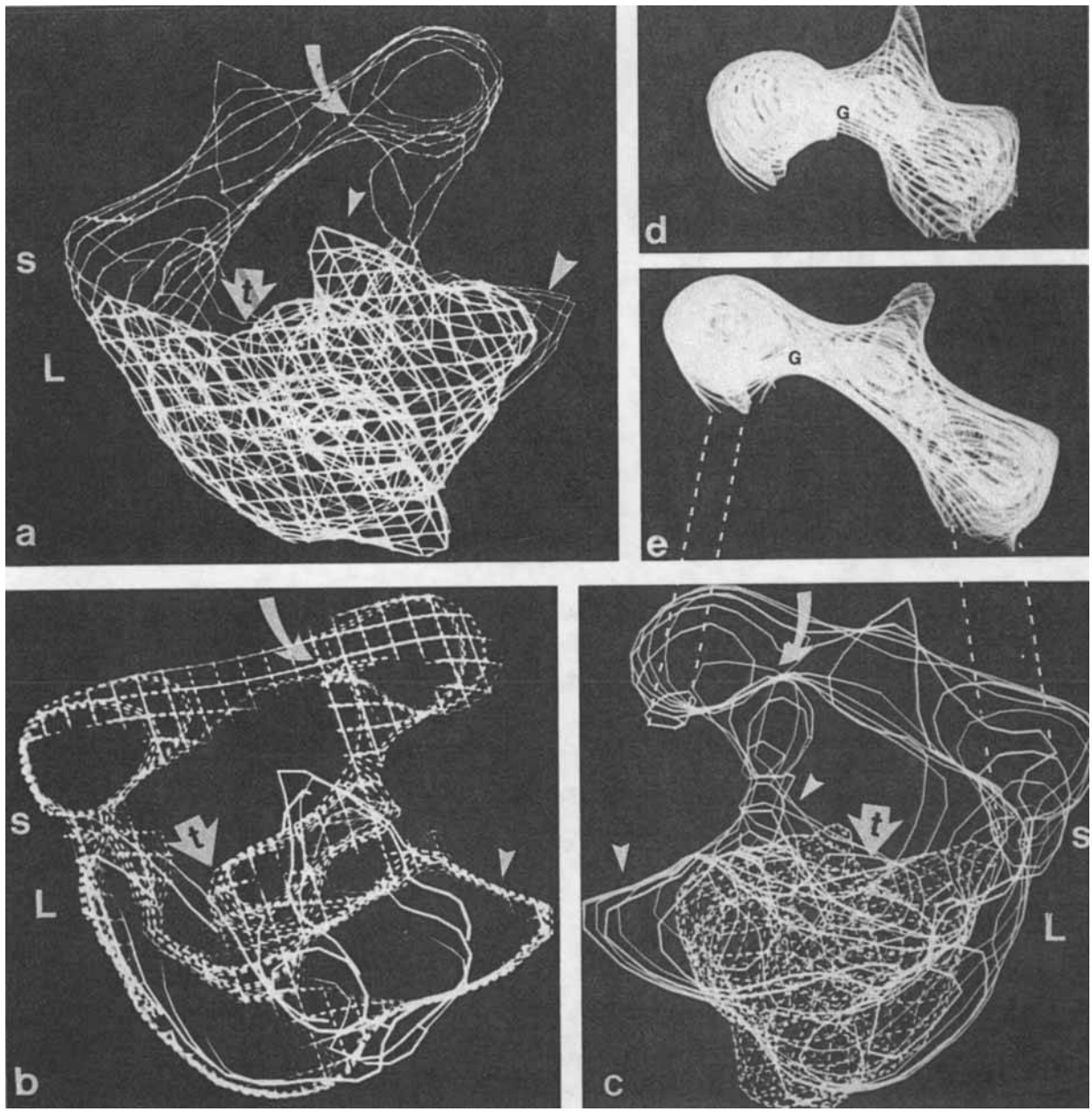

FIGURE 13. (a to c) Superpositions of computer graphic displays of the outline of the reconstructed models of 70S ribosome and the 50S ribosomal subunits. (b) shows a slice of the displayed model in (a) of 50 Å in depth. S and L mark the small and the large subunits, t shows the entrance to the tunnel. The arrow heads point at regions of extra density in the models of the 70S ribosomes, which may be a result of conformational changes of the large subunit upon their association to form 70S ribosomes. (d, e) show the outline of the 30S ribosomal subunit obtained by subtracting the density of the 50S subunit from that of the 70S ribosome. G and the curved arrows mark the groove, rich in RNA, in the small subunit.

estimated from tilted images of the sample. Since the range by which the sample can be tilted is limited by the geometry of the electron microscope, a significant amount of diffraction data cannot be collected (the "missing cone"). The missing data, in turn, led to a larger distortion of the reconstructed images in the direction perpendicular to the plane of the sheet. For this reason, it is generally assumed that the apparent depth of the sample in a reconstructed image may

be in error as high as 30%. In addition, elements of the structure along the c axis are more distorted than in the other directions.

In our reconstruction efforts we tried to account, as best as we could, for most of the limitations that are common to almost all the electron microscopical techniques, as well as to those that arise from the image-reconstruction procedures. To partially account for the shrinkage of the sample and the distortion of the images along the perpendicular direction, we compared the dimensions of reconstructed 70S ribosome with that of the 50S subunit. A reasonable fit between these two was obtained when the unit cell of the 70S particle was slightly expanded along one direction in the plane of the sheets and that of the 50S along the other one.[78] In this way, we accounted for the relative anisotropic shrinkage within planes of the two-dimensional arrays. Since there is no objective information about the shrinkage along the perpendicular axis (c), the least accurate one, and since the magnitude of the shrinkage implied by the above corrections was smaller than commonly observed in electron microscopic studies of biological samples the expansion applied to the reconstructed images along this direction was somewhat higher than that of the others. In parallel we attempt to obtain a more objective assessment of the size of the ribosome by comparing the results of three-dimensional image reconstruction with those obtained in X-ray and neutron crystallographic experiments.[33]

3. Neutron Diffraction

Single crystal neutron diffraction coupled with contrast variation may resolve the internal arrangements of selected components. This technique is based on the fact that the interactions of neutrons with atoms are not correlated with the number of electrons and therefore do not depend on the atomic numbers, as is the case for X-rays. In some cases, atoms with similar atomic numbers (e.g., the hydrogen atom and its isotope, deuterium) have very different scattering cross-sections for neutrons. Since ribosomes are composed of two distinctly different chemical entities, proteins and RNA chains, in principle it is possible to match the contrast (i.e., the diffracting power) of either of them with that of the solvent within the crystals by changing the relative concentrations of D_2O and H_2O in the solutions in which the crystals are immersed. In typical experiments, the diffraction is measured at a series of contrasts aimed at obtaining information about the relative distribution of the different ribosomal components. It is also possible, in principle, to use the contrast variation data to derive preliminary phase information.[96–98]

The main factor that limits the application of neutron diffraction of macromolecular crystals is the relatively poor diffracting power of biological crystals, a problem that is particularly acute for crystals of ribosomal particles. Many weeks or even months are required for data collection, even at low resolution, but since neutrons cause essentially no damage in the irradiated crystals measurements of such long durations are possible. Neutron diffraction data were collected and integrated to 30 Å resolution from crystals of 50S ribosomal subunits from *H. marismortui* (H50S(I)), and phase sets were generated using direct methods from normalized structure factors and selected by a sorting procedure.[33] The resulting map was relatively clean and contained several compact regions of density. A thorough examination of the map revealed that these compact features have a shape similar to those obtained by image reconstruction of the large subunit from *B. stearothermophilus* (Figure 12a and b and in References 13, 17, 75, and 78), but with slightly larger dimensions.[33]

V. FEASIBLE FUNCTIONAL RELEVANCES OF THE STRUCTURAL RESULTS

A. Preliminary Assignments of Functional Sites

As mentioned above, despite their low resolution, the models derived by image reconstruction from two-dimensional arrays displayed several structural features that had not been detected previously in prokaryotic ribosomes. Based on biochemical information we have suggested tentative functional roles for some of the features that were consistently observed in these recon-

structions. We should emphasize that an accurate determination of the shape and the size of the ribosomal particles, as well as a detailed assignment of functional sites, still await structural information of much higher resolution.

1. The Tunnel: a Plausible Path for the Nascent Protein

A prominent feature in the reconstructed models of both 70S ribosomes and 50S subunits from *B. stearothermophilus* is a tunnel spanning the 50S subunit of about 100 Å in length and up to 25 Å in diameter through the 50S subunit (Figures 12 and 13). Essentially the same tunnel has been found in all the reconstructions performed by us to date, regardless of whether gold thioglucose or uranyl acetate was used as the negatively staining agent. A similar feature was also apparent in filtered images of the same sheets viewed without stain in the electron microscope at cryotemperature.[13] A tunnel in the large ribosomal subunits is consistent with a feature revealed by image reconstruction of two-dimensional sheets of 80S eukaryotic ribosomes.[11] Recently, a similar feature was found in density maps computed from the neutron diffraction data from 50S subunits of *H. marismortui*.[33] In addition, hints for the existence of a series of internal cavities that may be linked to form an internal tunnel were detected at specific contouring level in ice-embedded single 50S subunits from *E. coli* that were subjected to sophisticated statistical three-dimensional image analysis.[99,100]

Although the tunnel is clearly visible in all our reconstructions of 50S particles,[13,17,75,78] it is somewhat less well resolved in reconstructions from two-dimensional arrays of assembled ribosomes.[11,13,17,77,78] This may be due, in part, to the lower resolution of the latter reconstructions. It is also conceivable that the tunnels of a large part of the 70S ribosomes in the crystallization samples are partially filled with fragments of nascent peptides, that remained bound during the purification and crystallization processes, causing a lower contrast between the tunnel and its surroundings, thus leading to difficulties in the detection of the tunnel. An additional feature that was observed in several reconstructions is a region of low density that branches off the main tunnel in the 50S subunit to form a Y- or V-shaped region of low density. In some reconstructions, this region appears to be of lower than average density, as found in boundaries between internal structural domains. In others, the density of this feature is as low as that of the tunnel itself and it appears to be a branch that leads to the opposite side of the particle.

A tunnel within the large ribosomal subunit that is spacious enough to accommodate the growing polypeptide was predicted more than 2 decades ago as a result of biochemical experiments that showed that the ribosome masks the nascent protein chains. In particular it was shown that the ribosome provides protection to the latest synthesized segments (25 to 40 amino acids) of the newly formed protein chains until the nascent protein is long enough to gain its own fold and develop its own resistance to proteolytic degradation.[14,44,101–106] The main tunnel described above may be a plausible exit pathway for the newly synthesized polypeptide explaining the observed masking of the ribosome for the following reasons:

1. The tunnel spans the 50S subunit, leading from the intersubunit space in the 70S ribosome, which we presumed to be the location of the peptidyl transferase site, to the other end of the 50S subunit at a location that may be compatible with the "exit" site of the nascent polypeptide chain, as identified by immune electron microscopy.[107]
2. The tunnel is long enough to accommodate a polypeptide chain of a length comparable to that found to be protected by the ribosome in any conformation.
3. The diameter of the tunnel, although rather ill defined due to the resolution limits, is wide enough to impose no obvious restrictions to the sequence of such peptides. There also appears to be enough room to accommodate amino acids to which bulky groups, such as biotin, are bound.[108]

Experiments performed in a number of laboratories have shown that the ability of the ribosome to protect a growing protein is sequence

independent. Besides naturally occurring proteins[101,103,105,106] and the polylysyl and polyphenylalanyl chains mentioned above, sequences rich in proline, obtained by translation of poly(C) or of the random copolymers (C,A) or (C,U), were also found to be protected by the ribosome.[14] Interestingly, polyproline is synthesized at a much lower rate than the other polypeptides, perhaps due to its more rigid conformation that may impose steric constraints in its propagation along the exit path.

Investigating the properties of the exit path of the nascent chains by identifying compounds that adhere to it should enable mapping the chemical environment of this path. We have begun such studies, having in mind the possibility of designing potential carriers for heavy-atom clusters that could form stable complexes with the ribosomal particles and that might be useful for phasing. As might be expected, various polypeptides differ in their ability to adhere to the ribosome. We have found that despite the excess positive charge of the ribosomal proteins, a newly formed chain of polylysine can be tightly bound to the large subunits of *B. stearothermophilus*[17,44] and of *H. marismortui*,[13,17,41] and even be co-crystallized together with them. These results suggest that the exit path of the nascent polypeptide may be composed, in part, by rRNA. In different experiments, newly synthesized chains of polyphenylalanine were found to bind to 50S subunits from *E. coli*[109] and to *B. stearothermophilus*,[13,17] suggesting that some regions of the exit path may be hydrophobic.

Immunoelectron microscopy showed that the N-terminus of nascent chains, encoded by either natural or artificial mRNA, can be detected in two distinct patches on the surface of the ribosome. One patch is close to the subunit interface, and the second is at the other end of the particle,[104] suggesting that the N-terminus might be exposed when only a few residues have been synthesized (on the first site), and when a longer chain is produced it emerges through the second site. These studies were extended further and refined, and in agreement with results of other experiments indicated that there are marked differences between the migration of nascent naturally occurring proteins and those coded by artificial messengers. It was also found that ribosomes protect natural proteins more efficiently than artificial homopolymers[106] and that homopolypeptides may choose a path slightly different than that of naturally occurring proteins.[110] It is conceivable that a common feature at the amino termini of natural proteins, such as the occurrence of f-Met as the terminal amino acid of prokaryotes, might have a role in guiding the nascent protein chain into the tunnel, presumably due to its high affinity for the entrance to the tunnel. Artificial proteins or homopolypeptides, lacking this feature of a natural amino terminus responsible for this affinity to the tunnel, may have smaller probability to enter the tunnel and thus may associate with other regions of the ribosome. Hence, during the initial stage of protein biosynthesis, the first few amino acids of the newly formed homopolypeptide may not enter the tunnel and thus could be exposed to antibodies or other chemical agents.[104,106]

If indeed the entry and the following transverse through the tunnel are essential for efficient protein biosynthesis, it is conceivable that the failure of newly synthesized chains to enter the tunnel is detected by the biosynthetic machinery at very early stages, leading to the termination of the process. This hypothesis may also explain why only 40 to 60% of a given population of ribosomes seem to be active in *in vitro* translation assays, when activity is defined as the production of relatively long chains, although almost all the ribosomes bind mRNA and tRNA.[45,111] The marked difference in the migration of short and long chains of newly synthesized polylysine and polyphenylalanine[110] can also be correlated with such mechanism. Thus, newly formed peptides that could not find their way into the tunnel may adhere to the surface of the ribosome according to their chemical properties and cause early termination of the biosynthetic pathway, whereas those that hit the right exit path continue to grow and migrate normally out of the ribosome.

In the absence of direct evidence, the hypothesis that the tunnel, revealed by image reconstruction, is the exit pathway of a nascent polypeptide, appears to provide a simple explanation for a number of properties of the ribosome. Since features corresponding to the tunnel have also been observed in eukaryotic ribosomes,[11] as well as in ribosomes of two radically different

bacteria, *B. stearothermophilus*,[75] a mild thermophilic eubacterium and *H. marismortui*,[33] an extreme halophilic archaebacterium, the tunnel and the functions associated with it are believed to be universal features of large ribosomal subunits.

2. A Low-Resolution Model for the 30S Subunit within the 70S Ribosome

As two-dimensional sheets of 30S subunits suitable for image reconstruction have not yet been grown, a directly reconstructed model of an isolated small subunit is still not available. However, by fitting the reconstructed model of the 50S subunit into that of the 70S ribosome, we were able to deduce the approximate shape of the small subunit as it appears within the 70S particle (Figure 13 and in Reference 78). The fitting was based on common structural elements in the models and on the orientation of the tunnel.

There is a significant similarity between the model of the small subunit obtained by this approach and that observed by visualization of single particles (for reviews see References 1, 2, and 90). Both are of similar volume; however, isolated 30S particles appear somewhat wider in electron micrographs and in reconstructions from single particles than in our model. The differences in the shapes may originate from artifacts such as flattening of the isolated particles on the grid, which are virtually eliminated in our two-dimensional sheets as, for our sheets, most of the contacts of the ribosomes with the electron microscope grid are through the 50S subunits. Alternatively, such differences could result from conformational changes in the subunits upon association to form a 70S ribosome.

3. The Intersubunit Space, a Plausible Binding Site for mRNA and tRNA

The small and large ribosomal subunits are well separated in our as well as in the other reconstructions of whole ribosomes regardless of the source of the ribosome, the preparative details, the stain, and the reconstruction procedure.[11,13,17,77,112] However, the empty space between the subunits, which is clearly resolved in our studies (Figures 11 to 13), is less well defined in the reconstructions from two-dimensional sheets of 80S ribosomes[11] and from averaged images of single 70S ribosomes.[112] It is likely that the poor definition of the empty space in the 80S ribosomes results from the lower resolution at which this reconstruction was performed. For the case of the single-particle reconstruction of the *E. coli* ribosome, this may originate from the collapse of the particles on the flat electron microscopical grid.[112] In our reconstructions the intersubunit free space comprises nearly 20% of the volume within the envelope of the 70S ribosome, and it is large enough to accommodate up to three tRNA molecules together with other factors of protein biosynthesis (see below, Section V.B). The intersubunit space is thus an obvious candidate for the location of the various enzymatic activities associated with the process of protein biosynthesis.

Uranyl acetate, which is commonly used as a negative stain for electron microscopy of biological specimens, acts in part as a positive stain and may be chemically incorporated into the ribosomal particles. Ribosomal RNA, the component most likely to interact chemically with uranyl acetate, can be detected by comparing reconstructed images obtained from two-dimensional arrays that have been stained by purely negative stain (e.g., gold thioglucose) and by uranyl acetate. In this way ribosomal-RNA-rich regions were detected at the interface of the small and the large subunits, in agreement with the results of the studies performed on unstained arrays of eukaryotic ribosomes.[11] Another RNA-rich region was found on the 30S subunit[13,17,77,78] in the vicinity of a groove that is clearly visible in the model derived from our reconstructions of the 70S particles (Figures 12 and 13). In accordance with biochemical and model-building experiments,[113] we have tentatively identified this groove as the mRNA binding site.

Spacial considerations allow the placement of a molecule of tRNA in the intersubunit space with its anticodon close to the mRNA binding site and its CCA-terminus positioned so that the peptidyl group may extend into the tunnel. In this orientation the tRNA molecule interacts with the walls of the intersubunit space; such interactions may account for noncognate affinity of the tRNA

to the ribosome. A speculative model building experiment in which a tRNA molecule[114] has been positioned in the intersubunit space is shown in Figure 14. The figure demonstrates that the intersubunit space is large enough to accommodate up to two more tRNA molecules, with some room left for other compounds, such as elongation factors.

The overall agreement in the shapes of the reconstructed model of the 50S subunit and that part of the reconstructed model of the 70S ribosome that was assigned as it is quite striking. However, there are two regions in which the two models differ slightly (Figure 13). At this stage it is not clear whether these differences reflect conformational changes occurring upon association of the subunits or whether they originate from differences in the resolutions of the two reconstructions (28 vs. 47 Å, for 50S and 70S, respectively).

B. The Design of Crystallizable Complexes That Mimic Ribosomes in Defined Functional States

We have attempted to form and crystallize complexes of whole 70S ribosomes and of its subunits with various nonribosomal cofactors and products of protein biosynthesis. These complexes were designed either to illuminate specific structural and functional features or to trap the ribosome in defined functional states. The design of these experiments was based on ideas derived from the model-building studies described above. The tentative assignment of the tunnel in the 50S subunit as the exit path of the nascent chain led to the crystallization of 50S subunits with a fragment of a newly formed polypeptide and a tRNA molecule (Table 1 and in References 13, 40, and 44). This complex yielded already small three-dimensional crystals, which may be used for elu-

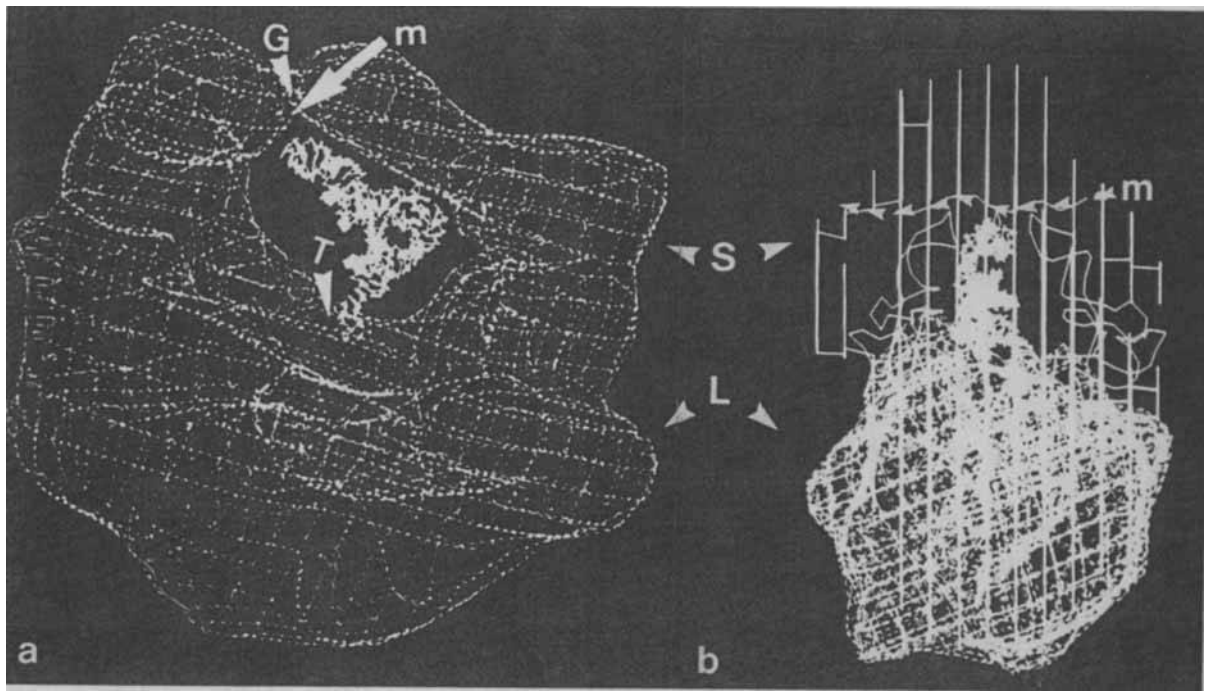

FIGURE 14. Two orthogonal views of the outline of the reconstructed model of 70S ribosome. The envelope of the 70S particle is shown as a dotted net on a, and as parallel lines on b. S and L indicate the small (30S) and the large (50S) subunits, respectively. G marks the groove rich in RNA in the small subunit, and T shows the entrance to the tunnel. "Model built" into the intersubunit free space are m, a piece of 28 ribonucleotides in an arbitrary conformation, which may simulate the mRNA chain (highlighted in b by arrowheads), together with three molecules of tRNA. Two of these tRNA molecules are shown as traces of their backbone. The tRNA molecule that points directly into the tunnel is highlighted by including all its atoms. For clarity we show in a only the highlighted tRNA molecule.

cidating the exit path taken by the newly formed protein chain.

In designing crystallizable complexes of the 70S ribosome, we assumed that the intersubunit space plays a major role in the conformational flexibility of the ribosome. Such flexibility may be crucial for the process of protein biosynthesis, but is an obstacle for the production of well-ordered crystals. It is most probable that the poor diffraction power and limited resolution of crystals of 70S ribosomes (Table 2) result from conformational heterogeneity in the sample. We have thus designed a series of complexes in which this conformational flexibility should be reduced, by the addition of components that are believed to bind in the intersubunit space, such as mRNA and tRNA.[78] For achieving this aim we attempted to select a combination of components that could lead to the formation of complexes that mimic natural steps in the process of protein biosynthesis.

A key component in all the complexes of this series is the mRNA. For obtaining stable complexes, this chain should have a high affinity for the ribosome and a sequence suitable for productive initiation of biosynthesis. At the same time, it should be short enough that its full length can be accommodated within the intersubunit space. It was clear from the outset that the production of such complexes in quantities suitable for crystallographic studies could present significant experimental difficulties. Thus, to assess the viability of this approach, we have designed a family of mRNA chains with increasing complexity.[115]

The simplest members in this series are homopolynucleotides of random lengths. Short homopolynucleotides with a defined length are somewhat more suitable. In preliminary crystallization experiments we used a complex composed of 70S ribosomes from *T. thermophilus* with an average of 1.5 to 1.8 equivalents of phetRNAphe and a short mRNA chain of about 35 uridyl residues. Crystals of this complex appear within 2 to 3 weeks as bipyramids with typical dimensions of 0.2 to 0.5 mm across (Figure 1 and in Reference 45).

It is noteworthy that the conditions for growing crystals of intact 70S ribosomes were found to be suitable also for growing crystals of this complex. However, crystals of the complex were obtained much more reproducibly than crystals of the 70S ribosome. The significant improvement in the reproducibility of the growth of crystals of the complex probably originates from the homogeneity of the crystallization mixture. It is conceivable that each preparation of 70S ribosomes includes some particles trapped in a rather rigid conformation, whereas others are devoided of any nonribosomal compound, and may assume higher flexibility. In these cases the crystallization process may involve the selection of ribosomes at similar, however not identical, conformations and the termination of crystal growth may be linked to the inclusion in the crystal ribosomal particles trapped in other conformational states. The observation that the crystals of the complex are isomorphous with those of the intact ribosomes supports this hypothesis.

Using well-defined starting solutions may also account for the marked improvement in the internal order of the crystals of the complex, compared with crystals of the 70S ribosome. This is further manifested by the higher resolution of the X-ray diffraction patterns collected from the crystals of the complex. Whereas crystals of 70S ribosomes diffract to 18 to 24 Å resolution at best, those of the complex diffract to better than 15 Å resolution.[45]

Our ultimate goal is the formation and the crystallization of stable complexes containing not only defined mRNA and tRNA components, but also a segment of a polypeptide chain. As mentioned above, we have already crystallized in two- and three-dimensions complexes of 50S subunits together with short chains of poly(Phe) or poly(Lys). Although these crystals are not yet suitable for crystallographic analysis, their mere existence encouraged us to design similar complexes of 70S ribosomes. We have initiated the production and the crystallization of complexes of 70S ribosomes together with heteronucleotides that code for desirable amino acid sequences, the corresponding charged tRNA molecules, and short segments of the nascent protein chain, ideally including a f-met residue as an amino-terminal and one or more cysteine residues to which heavy atoms could be covalently bound.

In order to estimate the individual contributions of the mRNA chain and the tRNA molecules to the stability and the rigidity of the com-

plex, we have attempted to cocrystallize 70S ribosomes together with oligo(U) of the same length used for the formation of the complex mentioned above. This led to occasional growth of poorly shaped crystals. Given the correlation between reproducibility of crystal growth and internal order seen for the other complex of T70S, it seems reasonable to conclude that the tRNA makes an important contribution to stabilizing the complex. The observation that crystals of complexes that more closely mimic a defined state in the process of protein biosynthesis are superior to those containing 70S ribosomes or those containing incomplete combinations of components encourages us to proceed along these lines.

VI. CONCLUDING REMARKS

The results reviewed in this article demonstrate that crystallographic studies on intact ribosomal particles are not only possible but well underway. From the early stages of this work, it has been clear that a straightforward application of the conventional techniques of macromolecular crystallography would not be adequate for the determination of the structures of ribosomal particles. Therefore, we have devised an approach that combines methods of macromolecular crystallography, electron microscopy, neutron diffraction, and cryotemperature techniques. We are also exploiting the extensive information available on the genetic and chemical properties of ribosomes for a rational design of derivatives of ribosomal particles using heavy-atom clusters.

This approach has enabled us to overcome a number of the difficulties associated with crystallographic analysis of ribosomal particles that a few years ago were thought to be insurmountable. Our broad-based approach, together with recent advances in the instrumentation for X-ray crystallography, leaves fewer conceptual obstacles to the determination of the three-dimensional structure of the ribosome, although a considerable amount of innovations, technical and computational developments, as well as tedious work remains to be done before our goal is achieved. In anticipation of a successful maturation of our efforts, we undertook crystallographic studies directed at the elucidation of the structures of ribosomes "trapped" in different functional states. We plan to use a number of static "snapshots" of this dynamic system to visualize the major conformational states of the ribosome and its subunits in the process of protein synthesis. In addition, since we obtain usable crystals of ribosomal particles from *B. stearothermophilus*, *T. thermophilus*, and *H. marismortui*, which represent both the eubacterial and archaebacterial kingdoms, we anticipate that results of our studies will not only reveal the structure of ribosomes but also will provide information about their evolution.

ACKNOWLEDGMENT

All stages of the studies presented here were carried out in active collaboration and under the inspiration and guidance of the late Prof. H. G. Wittmann.

This work was carried out at the Weizmann Institute of Science, the Max-Planck-Research-Unit at DESY in Hamburg, the Max-Planck-Institute for Molecular Genetics in Berlin, the EMBL Laboratory in Heidelberg, the ILL neutron diffraction facility in Grenoble, and at the following synchrotron facilities: EMBL/DESY, Hamburg; CHESS, Cornell University; SSRL, Stanford University; SRS, Daresbury, UK; and KEK, Japan.

Support was provided by the National Institute of Health (NIH GM 34360), the Federal Ministry for Research and Technology (BMFT 05 180 MP BO), the USA–Israel Binational Foundation (BSF 85-00381), the Kimmelman Center for Macromolecular Assembly at the Weizmann Institute, the Minerva and the Heinemann Foundations (4964 81). AY holds the Martin S. Kimmel Professorial chair.

REFERENCES

1. **Hardesty, B. and Kramer, G.,** *Structure, Function and Genetics of Ribosomes*, Springer-Verlag, Heidelberg, N.Y., 1986.
2. **Hill, E. W., Dahlbert, A., Garrett, R. A., Moore, P. B., Schlesinger, D., and Warner, J. R.,** *The*

Ribosomes: Structure, Function and Evolution, American Society for Microbiology, Washington, D.C., 1990.

3. **Bennett, W. and Huber,** Structure and function significance of domain motion in proteins, *Crit. Rev. Biochem.*, 15, 291, 1984.
4. **Kress, Y., Wittner, M., and Rosenbaum, R. M.,** Sites of cytoplasmic ribonucleoprotein-filament assembly in relation to helical body formation in axenic trophozoites of *Entamoeba histolytica*, *J. Cell Biol.*, 49, 773, 1971.
5. **Lake, J. A. and Slayter, H. S.,** Three-dimensional structure of the chromatoid body helix of entamoeba invades, *J. Mol. Biol.*, 66, 271, 1972.
6. **Unwin, P. N. T. and Taddei, C.,** Packing of ribosomes in crystals from the lizard Lacerta sicula, *J. Mol. Biol.*, 114, 491, 1977.
7. **Unwin, P. N. T.,** Attachment of ribosome crystals to intra cellular membranes, *J. Mol. Biol.*, 132, 69, 1979.
8. **O'Brien, L., Shelley, K., Towfighi, J., and McPherson, A.,** Crystalline ribosomes are present in brain of senile humans, *Proc. Natl. Acad. Sci. U.S.A.*, 77, 2260, 1980.
9. **Kuhlbrandt, W. and Unwin, P. N. T.,** Distribution of RNA and proteins in crystalline eukaryotic ribosomes, *J. Mol. Biol.*, 156, 611, 1982.
10. **Milligan, R. A. and Unwin, P. N. T.,** In vitro crystallization of ribosomes from chick embryos, *J. Cell. Biol.*, 95, 648, 1982.
11. **Milligan, R. A. and Unwin, P. N. T.,** Location of the exit channel for nascent proteins in 80S ribosomes, *Nature*, 319, 693, 1986.
12. **Yonath, A. and Wittmann, H. G.,** Crystallographic and image reconstruction studies on ribosomal particles from bacterial sources, in *Methods in Enzymology*, Moldave, K. and Noller, H., Eds., Academic Press, 1988, 95.
13. **Yonath, A., Bennett, W., Weinstein, W., and Wittmann, H. G.,** Crystallography and image reconstruction of ribosomes, cited from Reference 2.
14. **Evers, U. and Gewitz, H. G.,** Studies on the accessibility of nascent non-helical peptide chains on the ribosomes, *Biochem. Int.*, 19, 1031, 1989.
15. **Glotz, C., Müssig, J., Gewitz, H.-S., Makowski, I., Arad, T., Yonath, A., and Wittmann, H. G.,** Three-dimensional crystals of ribosomes and their subunits from eu-, and archaebacteria, *Biochem. Int.*, 15, 953, 1987.
16. **Yonath, A., Glotz, C., Gewitz, H. S., Bartels, K., von Böhlen, K., Makowski, I., and Wittmann, H. G.,** Characterization of crystals of small ribosomal subunits, *J. Mol. Biol.*, 203, 831, 1988.
17. **Yonath, A. and Wittmann, H. G.,** Challenging the three-dimensional structure of ribosomes, *TIBS*, 14, 329, 1989.
18. **Trakhanov, S. D., Yusupov, M. M., Agalarov, S. C., Garber, M. B., Ryazantsev, S. N., Tischenko, S. V., and Shirokov, V. A.,** Crystallization of 70S ribosomes and 30S ribosomal subunits from *Thermus thermophilus*, *FEBS Lett.*, 220, 319, 1987.
19. **Yusupov, M. M., Tischenko, S. V., Trakhanov, S. D., Ryazantsev, S. N., and Garber, M. B.,** A new crystalline form of 30S ribosomal subunits from *Thermus thermophilus*, *FEBS Lett.*, 238, 113, 1988.
20. **Yonath, A., Müssig, J., and Wittmann, H. G.,** Parameters for crystal growth of ribosomal subunits, *J. Cell. Biochem.*, 19, 629, 1982.
21. **Miskin, R., Zamir, A., and Elson, D.,** Inactivation and reactivation of ribosomal subunits: the peptidyl transferase activity of the 50S subunit of *E. coli*, *J. Mol. Biol.*, 54, 355, 1978.
22. **Yonath, A., Müssig, J., Tesche, B., Lorenz, S., Erdmann, V. A., and Wittmann, H. G.,** Crystallization of the large ribosomal subunit from *B. stearothermophilus*, *Biochem. Int.*, 1, 428, 1980.
23. **Yonath, A., Khavitch, G., Tesche, B., Müssig, J., Lorenz, S., Erdmann, V. A., and Wittmann, H. G.,** The nucleation of crystals of the large ribosomal subunits from *B. stearothermophilus*, *Biochem. Int.*, 5, 629, 1982.
24. **Gibbs, J. W.,** *Collected Works of J. W. Gibbs*, Longmas Green, New York, 1928, 55.
25. **Zettlemoyer, A. C.,** *Nucleation*, Marcel Dekker, New York, 1969.
26. **Kam, Z., Shore, A. B., and Feher, G.,** On the crystallization of proteins, *J. Mol. Biol.*, 123, 539, 1978.
27. **Trakhanov, S. D., Yusupov, M. M., Shirokov, V. A., Garber, M. B., Mitschler, A., Ruff, M., Thierry, J.-C., and Moras, D.,** Preliminary X-ray investigation of 70S ribosome crystals from *E. coli*, *J. Mol. Biol.*, 209, 327, 1989.
28. **Berkovitch-Yellin, Z., Hansen, H., Bennett, W. S., Sharon, R., von Böhlen, K., Volkmann, N., Piefke, J., Yonath, A., and Wittmann, H. G.,** Crystals of 70S ribosomes from thermophilic bacteria are suitable for X-ray analysis at low resolution, *J. Crystal Growth*, 110, 208, 1991.
29. **Wittmann, H. G., Müssig, J., Gewitz, H. S., Piefke, J., Rheinberger, H. J., and Yonath, A.,** Crystallization of *E. coli* ribosomes, *FEBS Lett.*, 146, 217, 1982.
30. **Wittmann, H. G. and Yonath, A.,** Diffraction studies on crystals of ribosomal particles, in *The Structure and Function of the Genetic Apparatus*, Ts'o and Nicollini Eds., Plenum Press, 1985, 177.
31. **Schnier, J., Gewitz, H. S., Behrens, E., Lee, A., Ginther, G., and Leighton, T.,** Isolation and characterization of *Bacillus stearothermophilus* 30S and 50S ribosomal protein mutations, *J. Bacteriol.*, 172, 7306, 1990.
32. **Weinstein, S., Jahn, W., Wittmann, H. G., and Yonath, A.,** Novel procedures of derivatization of ribosomes for crystallographic studies, *J. Biol. Chem.*, 264, 19138, 1989.

33. **Eisenstein, M., Sharon, R., Berkovitch-Yellin, Z., Gewitz, H.-S., Weinstein, S., Pebay-Peyroula, E., Roth, M., and Yonath, A.,** The interplay between X-ray crystallography, neutron diffraction, image reconstruction, organo-metallic chemistry and biochemistry in structural studies of ribosomes, *Biochemie*, 73, 897, 1991.
34. **Yonath, A., Tesche, B., Lorenz, S., Müssig, J., Erdmann, V. A., and Wittmann, H. G.,** Several crystal forms of the 50S ribosomal particles of *Bacillus stearothermophilus, FEBS Lett.*, 154, 15, 1983.
35. **Yonath, A., Bartunik, H. D., Bartels, K. S., and Wittmann, H. G.,** Some X-ray diffraction patterns from single crystals of the large ribosomal subunits from *B. stearothermophilus, J. Mol. Biol.*, 177, 201, 1984.
36. **Yonath, A., Saper, M. A., Makowski, I., Müssig, J., Piefke, J., Bartunik, H. D., Bartels, K. S., and Wittmann, H. G.,** Characterization of single crystals of the large ribosomal particles from *B. stearothermophilus, J. Mol. Biol.*, 187, 633, 1986.
37. **Yonath, A., Saper, M. A., and Wittmann, H. G.,** Structural studies on ribosomal particles, cited from Reference 1.
38. **Yonath, A., Saper, M. A., Frolow, F., Makowski, I., and Wittmann, H. G.,** Characterization of single crystals of large ribosomal particles from a mutant of *B. stearothermophilus, J. Mol. Biol.*, 192, 161, 1986.
39. **Yonath, A.,** Three-dimensional crystals of ribosomal particles, *TIBS*, 9, 227, 1984.
40. **Müssig, J., Makowski, I., von Böhlen, K., Hansen, H., Bartels, K. S., Wittmann, H. G., and Yonath, A.,** Crystals of wild-type, mutated, derivatized and complexed 50S ribosomal subunits from *Bacillus stearothermophilus* suitable for X-ray analysis, *J. Mol. Biol.*, 205, 619, 1989.
41. **Yonath, A., Leonard, K. R., Weinstein, S., and Wittmann, H. G.,** Approaches to the determination of the three-dimensional architecture of ribosomal particles, in *Cold Spring Harbor Symposium on Quantum Molecular Biology*, Vol. 52, Watson, J., Ed., 1987, 729.
42. **Yonath, A. and Wittmann, H. G.,** Approaching the molecular structure of ribosomes, *J. Biophys. Chem.*, 29, 17, 1988.
43. **Yonath, A., Frolow, F., Shoham, F., Müssig, J., Makowski, I., Glotz, C., Jahn, W., Weinstein, S., and Wittmann, H. G.,** Crystallography of ribosomes, *J. Crystal Growth*, 90, 231, 1988.
44. **Gewitz, H. S., Glotz, C., Piefke, J., Yonath, A., and Wittmann, H. G.,** Two-dimensional crystalline sheets of the large ribosomal subunits containing the nascent protein chain, *Biochimie*, 70, 645, 1988.
45. **Hansen, H., Volkmann, N., Piefke, J., Glotz, C., Weinstein, S., Makowski, I., Meyer, S., Wittmann, H. G., and Yonath, A.,** Crystals of complexes mimicking protein biosynthesis are suitable for crystallographic studies, *Biochem. Biophys. Acta*, 1050, 1, 1990.
46. **Volkmann, N., Hottentrager, S., Hansen, H., Zayzsev-Bashan, A., Sharon, R., Berkovitch-Yellin, Z., Yonath, A., and Wittmann, H. G.,** Characterization and preliminary crystallographic studies on large ribosomal subunits from *Thermus thermophilus, J. Mol. Biol.*, 216, 239, 1990.
47. **Shevack, A., Gewitz, H. S., Hennemann, B., Yonath, A., and Wittmann, H. G.,** Characterization and crystallization of ribosomal particles from halobacterium marismotoui, *FEBS Lett.*, 184, 68, 1985.
48. **Shoham, M., Müssig, J., Shevack, A., Arad, T., Wittmann, H. G., and Yonath, A.,** A new crystal form of large ribosomal subunits from *Halobacterium marismortui, FEBS Lett.*, 208, 321, 1986.
49. **Makowski, I., Frolow, F., Saper, M. A., Wittmann, H. G., and Yonath, A.,** Single crystals of large ribosomal particles from *Halobacterium marismortui* diffract to 6 Å, *J. Mol. Biol.*, 193, 819, 1987.
50. **von Böhlen, K., Bartels, H., Hansen, H., Makowski, I., Meyer, S., Franceschi, F., and Yonath, A.,** Single crystals of large ribosomal particles from *Halobacterium marismortui* diffract to 3 Å, *J. Mol. Biol.*, 221, 11, 1991.
51. **Sussman, J. L., Zippori, Z., Harel, M., Yonath, A., and Werber, M. M.,** Preliminary X-ray diffraction studies on 2 Fe-ferredoxin from Halobacterium of the Dead Sea, *J. Mol. Biol.*, 134, 375, 1979.
52. **Harel, M., Shoham, M., Frolow, F., Eisenberg, H., Mevarech, M., Yonath, A., and Sussman, J. L.,** Crystallization of halophilic malate dehydrogenase from *Halobacterium marismortui, J. Mol. Biol.*, 200, 609, 1988.
53. **Arad, T., Leonard, K. R., Wittmann, H. G., and Yonath, A.,** Two-dimensional crystalline sheets of *B. stearothermophilus* ribosomal particles, *EMBO J.*, 3, 127, 1984.
54. **McPherson, A., Koszelak, S., Axelrod, H., Day, J., Williams, R., Robinson, L., McGrath, M., and Cascio, D.,** An experiment regarding crystallization of soluble proteins in the presence of beta-octyl glucoside, *J. Biol. Chem.*, 261, 1969, 1986.
55. **Berkovitch-Yellin, Z., van Mil, J., Addadi, L., Idelson, M., and Leiserorowitz, L.,** Crystal morphology by tailor-made inhibitors: a new probe for fine intermolecular interactions, *J. Am. Chem. Soc.*, 107, 3111, 1985.
56. **Bartels, K. S., Weber, G., Weinstein, S., Wittmann, H. G., and Yonath, A.,** Synchrotron light on ribosomes: the development of crystallographic studies of bacterial ribosomal particles, in *Chemical and Biological Applications of Synchrotron Radiation*, Vol. 2, Mandelkow, E., Ed., part of *Topics in Current Chemistry*, Vol. 147, Springer-Verlag, Heidelberg, 1988, 58.
57. **Klug, A., Holmes, K. C., and Finch, J. T.,** X-ray diffraction studies on ribosomes from different sources, *J. Mol. Biol.*, 3, 87, 1961.

58. **Langridge, R. and Holmes, K. C.,** X-ray diffraction studies of concentrated gels of ribosomes from *E. coli, J. Mol. Biol.*, 5, 611, 1962.
59. **Zubay, G. and Wilkins, M. H. F.,** X-ray diffraction studies of the structure of ribosomes from *E. coli, J. Mol. Biol.*, 2, 105, 1960.
60. **Hope, H.,** Cryocrystallography of biological macromolecules: a generally applicable method, *Acta Cryst.*, B44, 22, 1988.
61. **Hope, H., Frolow, F., von Böhlen, K., Makowski, I., Kratky, C., Halfon, Y., Danz, H., Webster, P., Bartels, K., Wittmann, H. G., and Yonath, A.,** Cryocrystallography of ribosomal particles, *Acta Cryst.*, B45 (345), 190, 1989.
62. **Hartmann, H., Parak, F., Steigemann, W., Petsko, G. A., Ringe Ponzi, D., and Frauenfelder, H.,** Conformational substates in a protein structure and dynamics of metmyoglobin at 80 K, *Proc. Natl. Acad. Sci. U.S.A.*, 79, 4967, 1982.
63. **Petsko, G. A.,** Protein crystallography at subzero temperatures: cryoprotective liquors for protein crystals, *J. Mol. Biol.*, 96, 381, 1975.
64. **Bellon, P., Manassero, M., and Sansoni, M.,** Crystal and molecular structure of tri-iodoheptakis (tri-*p*-fluorophenyl phosphine) undecagold, *J. Chem. Soc. Dalton Trans.*, 1481, 1972.
65. **Jahn, W.,** Synthesis of water soluble undecagold cluster for specific labeling of proteins, *Z. Naturforsch.*, 44b, 1313, 1989.
66. **Jahn, W.,** Synthesis of water soluble tetrairidium clusters suitable for heavy atom labeling of proteins, *Z. Naturforsch.*, 44b, 79, 1989.
67. **Crick, F. H. C. and Magdoff, B. S.,** The theory of the method of isomorphous replacement for protein crystals, *Acta. Cryst.*, 9, 901, 1956.
68. **Carazo, J. M., Wagenknecht, T., Radermacher, M., Mandiyan, V., Boublik, M., and Frank, J.,** Three-dimensional structure of 50S *E. coli* subunit depleted of protein L7/L12, *J. Mol. Biol.*, 201, 393, 1988.
69. **Gewitz, H.-S., Glotz, C., Goischke, P., Romberg, B., Müssig, J., Yonath, A., and Wittmann, H. G.,** Reconstitution and crystallization experiments with isolated split proteins from *Bacillus stearothermophilus* ribosomes, *Biochem. Int.*, 15, 887, 1987.
70. **Sanchez, M. E., Urena, D., Amils, R., and Londei, P.,** *In vitro* reassembly of active large ribosomal subunits of the halophilic archaebacterium *Halogax mediterrane, Biochemistry*, 29, 9256, 1990.
71. **Koepke, A. K. E., Paulke, C., and Gewitz, H.-S.,** Overexpression of Methanococcal ribosomal protein L12 in *E. coli* and its incorporation into Halobacterial 50S subunits yielding active ribosomes, *J. Biol. Chem.*, 265, 6436, 1990.
72. **Nierhaus, K. K., Brimacombe, R., and Wittmann, H. G.,** Inhibition of protein biosynthesis by antibiotics, in *Perspectives in Antiinfective Therapy* Jackson, G. G., Schlumberger, H. D., and Zeiler, H. J., Eds., Friedr. Vieweg and Sohn Braunschweig/Wiesbaden, 1989, 29.
73. **Hill, W. E., Trappich, B. E., and Tassanakajohn, B.,** Probing ribosomal structure and function, cited in Reference 1.
74. **Hill, W. E., Weller, J., Gluick, T., Merryman, C., Marconi, R. T., Tassanakajohn, A., and Trappich, W. E.,** Probing ribosomal structure and function by using short complementary DNA oligomers, cited from Reference 2.
75. **Yonath, A., Leonard, K. R., and Wittmann, H. G.,** A tunnel in the large ribosomal subunit revealed by three-dimensional image reconstruction, *Science*, 236, 813, 1987.
76. **Arad, T., Piefke, J., Gewitz, H. S., Hennemann, B., Glotz, C., Müssig, J., Yonath, A., and Wittmann, H. G.,** The growth of ordered two-dimensional sheets of ribosomal particles from salt-alcohol mixtures, *J. Analytical Biochem.*, 167, 113, 1987.
77. **Arad, T., Piefke, J., Weinstein, S., Gewitz, H. S., Yonath, A., and Wittmann, H. G.,** Three-dimensional image reconstruction from ordered arrays of 70S ribosomes, *Biochimie*, 69, 1001, 1987.
78. **Berkovitch-Yellin, Z., Wittmann, H. G., and Yonath, A.,** Low resolution models for ribosomal particles reconstructed from electron micrographs of tilted two-dimensional sheets: tentative assignments of functional sites, *Acta Cryst.*, B46, 637, 1990.
79. **Leijonmarck, M., Eriksson, S., and Liljas, A.,** Crystal structure of a ribosomal component at 2.6 Å resolution, *Nature*, 286, 824, 1980.
80. **Appelt, K., Kijk, J., Reinhardt, R., Sanhuesa, S., White, S. W., Wilson, K. S., and Yonath, A.,** The crystallization of ribosomal proteins from the 50S subunit of the *E. coli* and *B. stearothermophilus* ribosome, *J. Biol. Chem.*, 256, 11787, 1981.
81. **Liljas, A. and Newcomer, M. E.,** Purification and crystallization of a protein complex from *Bacillus stearothermophilus* ribosome, *J. Mol. Biol.*, 153, 393, 1981.
82. **Appelt, K., Dijk, J., White, S. T., Wilson, K. S., and Bartels, K.,** Protein of the *Bacilus stearothermophilus*: a low resolution crystal analysis of protein L30, *FEBS Lett.*, 160, 72, 1983.
83. **Appelt, K., Dijk, J., White, S. T., and Wilson, K. S.,** Proteins of *Bacilus stearothermophilus* ribosome: crystallization of protein L6, *FEBS Lett.*, 160, 75, 1983.
84. **Moore, P. B., Kime, M. J., Leontis, N. B., and Abdel-Meguid, S. S.,** Physical studies on a nucleoprotein from the ribosome of *E. coli, J. Biomolec. Struct.& Dynam.*, 1, 383, 1983.
85. **Sedelnikova, S. E., Agalarov, S. Ch., Garber, M. B., and Yusupov, M. M.,** Proteins of the *Thermus thermophilus* ribosome: purification of several individual proteins and crystallization of protein TL7, *FEBS Lett.*, 238, 113, 1989.

86. **Agalarov, S.Ch., Eliseikina, I. A., Sedelnikova, S. E., Fomenkova, N. P., Nikonov, S. V., and Garber, M. B.,** Crystals of protein L1 from the 50S ribosomal subunit of *Thermus thermophilus*. Preliminary crystallographic data, *J. Mol. Biol.*, 216, 501, 1990.
87. **Sedelnikova, S. E., Agalarov, S.Ch., Eliseikina, I. A., Fomenkova, N. P., Nikonov, S. V., Garber, M. B., Svensson, A., and Liljas, A.,** Preliminary crystallographic studies on protein L6 from the large ribosomal subunits of *Thermus thermophilus*, *J. Mol. Biol.*, in press.
88. **Leonard, K. R., Arad, T., Tesche, B., Erdmann, V. A., Wittmann, H. G., and Yonath, A.,** Crystallization, electron microscopy and three-dimensional reconstruction studies of ribosomal subunits, in *Electron Microscopy 1982*, Vol. 3, Offizin Paul Hartung, Hamburg, 1982, 9.
89. **Stuhrmann, H. B., Haas, J., Ibel, K., De Wolf, B., Koch, M. H. J., Parfait, R., and Chrichton, R. R.,** New low resolution model of 50S of *E. coli* ribosomes, *Proc. Natl. Acad. Sci. U.S.A.*, 2379, 1976.
90. **Wittmann, H. G.,** Architecture of prokaryotic ribosomes, *Annu. Rev. Biochem.*, 52, 35, 1983.
91. **Lake, J.,** Ribosome structural and functional sites, in *Ribosomes Structure, Function and Genetics*, Chambliss et al., Eds., University Park Press, Baltimore, 1979, 201.
92. **Clark, W., Leonard, K., and Lake, J.,** Ribosomal crystalline arrays of large subunits from *E. coli*, *Science*, 216, 999, 1982.
93. **Oakes, M., Henderson, E., Scheiman, A., Clark, M., and Lake, J.,** Ribosome structure, function and evolution: mapping ribosomal RNA, proteins and functional site in three dimensions, cited from Reference 1.
▶94. **Piefke, J., Arad, T., Gewitz, H. S., Yonath, A., and Wittmann, H. G.,** The growth of ordered two-dimensional sheets of whole ribosomes from *B. stearothermophilus*, *FEBS Lett.*, 209, 104, 1986.
95. **Shirokov, V. A., Ryazantsev, S. N., Sergeev, Y. V., Garber, M. B., and Vasiliev, V. D.,** Thin laminar microcrystals of 70S ribosomes from *Thermus thermophilus*, *FEBS Lett.*, 258, 147, 1989.
96. **Roth, M., Lewit-Bentley, A., Michel, H., Deisenhofer, J., Huber, R., and Oesterheld, D.,** Detergent structure in crystals of a bacterial photosynthetic reaction center, *Nature*, 340, 659, 1989.
▶97. **Podjarny, A., Rees, B., Thierry, J. C., Cavarelli, J., Jesior, J. C., Roth, M., Lewit-Bentley, A., Kahn, R., Lorber, B., Ebel, J. P., Giege, R., and Moras, D.,** Yeast TRNAasp-aspartyl-tRNA synthetase complex: low resolution crystal structure, *J. Biomol. Struct., Dynamic*, 5, 187, 1987.
▶98. **Bentley, G. A., Lewit-Bentley, A., Liljas, L., Skoglund, U., Roth, M., and Unge, T.,** Structure of RNA il satellite tobacco necrosis virus a low resolution neutron diffraction study using 1H20/2H20 solvent contrast variation, *J. Mol. Biol.*, 194, 129, 1987.
99. **Wagenknecht, T., Graassucc, R., and Frank, J.,** Electron microscopy and computer image averaging of ice-embedded large ribosomal subunits from *E. coli*, *J. Mol. Biol.*, 199, 137, 1988.
100. **Frank, J., Verschoor, A., Radamaacher, M., and Wagenknecht, T.,** Morphologies of eubacterial and eukaryotic ribosomes as determined by three dimensional electron microscopy, cited from Reference 2.
101. **Malkin, L. I. and Rich, A.,** Partial resistance of nascent polypeptide chains to proteolytic digestion due to ribosomal shielding, *J. Mol. Biol.*, 26, 329, 1967.
▶102. **Blobel, G. and Sabatini, D. D.,** Controlled proteolysis of nascent polypeptides in rat liver cell fractions, *J. Cell Biol.*, 45, 130, 1970.
103. **Smith, W. P., Tai, P. C., and Davis, B. D.,** Interaction of secreted nascent chains and surrounding membranes in *Bacillus subtilis*, *Proc. Natl. Acad. Sci. U.S.A.*, 75, 5922, 1978.
104. **Ryabova, L. A., Selivanova, O. M., Baranov, V. I., Vasiliev, V. D., and Spirin, A. S.,** Does the channel for nascent peptide exist inside the ribosome?, *FEBS Lett.*, 226, 255, 1988.
105. **Yen, I. J., Macklin, P. S., and Cleavland, D. W.,** Autoregulated instability of beta-tubulin mRNAs by recognition of the nascent amino terminus of beta-tubulin, *Nature*, 334, 580, 1988.
106. **Kolb, V. A., Kommer, A., and Spirin, A. S.,** Nascent peptide and the ribosomal tunnel, Workshop on Translation, Leiden, p.84a.
107. **Barnebeu, C. and Lake, J. A.,** Nascent polypeptide chains emerge from the exit domain of the large ribosomal subunit: immune mapping of the nascent chain, *Proc. Natl. Acad. Sci. U.S.A.*, 79, 3111, 1982.
▶108. **Kurzchalia, S. V., Wiedmann, M., Breter, H., Zimmermann, W., Bauschke, E., and Rapoport, T. A.,** tRNA-mediated labeling of proteins with biotin, a nonradioactive method for the detection of cell-free translation products, *Eur. J. Biochem.*, 172, 663, 1988.
109. **Gilbert, W.,** Protein synthesis in *E. coli*, *Cold Spring Harbor Symp. Quantitative Biol.*, 28, 287, 1963.
110. **Hardesty, B., Picking, W. D., and Odom, O. W.,** The extension of polyphenyl alanynine and poly lysine peptides on *E. coli* ribosomes, *Biochem. Biophys. Acta*, 1050, 197, 1990.
111. **Rheinberger, H.-J. and Nierhaus, K. H.,** Partial release of AcPhe2-tRNA from ribosome during poly(u) dependent poly(phe) synthesis and the effects of chloramphenicol, *Eur. J. Biochem.*, in press.
112. **Wagenknecht, T., Carazo, J. M., Radermacher, M., and Frank, J.,** Three-dimensional reconstruction of the ribosome from *E. coli*, *Biophys. J.*, 55, 455, 1989.
113. **Brimacombe, R., Atmadja, J., Stiege, W., and Schueler, D.,** A detailed model of the three-dimen-

sional structure of *E. coli* 16S ribosomal RNA *in situ* in the 30S subunit, *J. Mol. Biol.*, 199, 115, 1988.
114. **Sussman, J. L., Holbrook, S. R., Warrent, W. R., Church, G. M., and Kim, S. H.,** Crystal structure of yeast phenylalanine transfer RNA. I. Crystallographic refinement, *J. Mol. Biol.*, 123, 607, 1978.
115. **Evers, U., Triana, F., Nierhaus, K., and Yonath, A.,** Crystallographic studies on complexes mimicking protein biosynthesis, *Biol. Chem. Hoppe-Seyler*, 371, 782, 1990.
116. **Eilam, Y., Elson, D., and Danon, D.,** unpublished data.
117. **Arndt, E., Franceschi, F., Mevarech, M., Kruft, V., and Yonath, A.,** unpublished.
118. **Glotz, C., Yonath, A., and Wittmann, H. G.,** unpublished data.
119. **Evers, U. and Yonath, A.,** unpublished.
120. **Leonard, K., Arad, T., Yonath, A., and Wittmann, H. G.,** unpublished.
121. **Piefke, J., Yonath, A., and Wittmann, H. G.,** unpublished.
122. **Leonard, K. R., Arad, T., Piefke, J., and Yonath, A.,** unpublished.